5-2010

TIME-DEPENDENT SCOUR DEPTH UNDER BRIDGE-SUBMERGED FLOW

Yuan Zhai
University of Nebraska - Lincoln, 43michelle@gmail.com

TIME-DEPENDENT SCOUR DEPTH UNDER BRIDGE-SUBMERGED FLOW

by

Yuan Zhai

A THESIS

Presented to the Faculty of

The Graduate College at the University of Nebraska

In Partial Fulfillment of Requirements

For the Degree of Master of Science

Major: Civil Engineering

Under the Supervision of Professor Junke Guo

Lincoln, Nebraska

May, 2010

TIME-DEPENDENT SCOUR DEPTH UNDER BRIDGE-SUBMERGED FLOW

Yuan Zhai, M.S.

University of Nebraska, 2010

Advisor: Junke Guo

Failure of bridges due to local scour has motivated many investigators to explore the reasons of scouring and to give the prediction of the scour depth. But most scour prediction equations only address non-pressure-flow situations. Little research has been dedicated to another destructive scour, submerged-flow bridge scour (pressure flow scour) which can cause significant damages to bridges when partially or totally submerged during a large flood.

This thesis is specifically focused on the experimental study for time-dependent scour depth under bridge-submerged flow. The experiments were conducted in a self contained re-circulating tilting flume where two uniform sediment sizes and one model bridge deck with three different inundation levels were tested for scour morphology. To this end, a semi-empirical model for estimating time-dependent scour depth was then presented based on the mass conservation of sediment, which agrees very well with the collected data.

As current practice for determining the scour depth at a bridge crossing is based on the equilibrium scour depth of a design flood (e.g., 50-year, 100-year, and 500-year flood events), which is unnecessarily larger than a real maximum scour depth during a bridge life span since the peak flow period of a flood event is often much shorter than the corresponding scour equilibrium time. The proposed method can appropriately reduce the design depth of bridge scour according to design flow and a peak flow period, which can translate into significant savings in the construction of bridge foundations.

ACKNOWLEDGEMENTS

I would like to express my thanks to all those who have instructed and helped me with this thesis.

First of all, I wish to express my heartfelt gratefulness to my advisor Dr. Junke Guo for the invaluable guidance, positive encouragement and patience he provided to me during the period of the research and the thesis writing process. His wealth of knowledge and enthusiasm to share them with me is most appreciated. I have furthermore to appreciate Dr. Kornel Kerenyi, Research Manager of the FHWA Hydraulics R&D Program, provided the experimental data that were very important for this research, as well as Dr.Lianjun Zhao, whom I worked with for experiments and data collections. Thanks also go to my classmates, Mr. Haoyin Shan, Mr. Zhaoding Xie and Ms. Afzal Bushra, for discussing the issues and solutions of my research.

Finally, I am greatly indebted to my parents for their love and support. Without their many years of encouragement and support, I may never reach where I am today.

TABLE OF CONTENTS

LIST OF TABLES

LIST OF FIGURES

Chapter 1 Introduction

1.1 Research Background

As a vital component of the transportation network, bridges play a pivotal role in modern society. A bridge is a structure built to span a valley, road, body of water, or other physical obstacle, for the purpose of providing passage over the obstacle. Approximately 84 percent of the bridges are over water bodies, like a river, creek, lake and ocean (NCHRP Report 396, 1997). Scour, defined as "the erosion or removal of streambed or bank material form bridge foundations due to flowing water" is the most common cause of the highway bridge failures in the United States (Kattell & Eriksson, 1998). According to statistic, 60% of all bridge failures result from scour and other hydraulic related causes. In this regard, scour is the primary cause of bridge failure in the United States (NCHRP Report 396, 1997).

Figure 1.1 Little Salmon River Bridge, Nez Perce National Forest. A January 1997 flood event scoured the abutment and one of the intermediate piers causing failure (Kattell & Eriksson,1998)

Although scour may occur at any time, scour action is especially strong during floods. Scour of the streambed near the bridge piers and abutments led to more bridge failures than other causes in the history (Murillo, 1987). D.W.Smith (1976), who is a British bridge engineer, did an analysis about the failure reasons of the 143 damaged bridges during the year of 1847 to 1975. The conclusion is displayed in the Table 1.1.

Table 1.1 Word-wide bridge failures categories (1847~1975) (D.W. Smith 1976)

Classification	Reasons	Number
1	Flood scour	70
2	Inappropriate materials	22
3	Overloading and Accidents	14
4	Inappropriate installment	12
5	Earthquakes	11
6	Error in design	5
7	Wind Destroy	4
8	Fatigue	4
9	Rust	1

With the high incidence of bridge failures due to flood scour, many have become disturbed and alarmed. Bridge scour often resulted in substantial interruption of traffic, and sometimes loss of life, not to mention damage to vehicles. Reviewing the past twenty years, the bridge accidents resulted from flood scouring occurred all over the world. Scour at bridges is a problem of national scope and is not limited to a few geographical areas (Table 1.2)(David, 2000). In Great Britain, a bridge over river Crane near Feltham,

partially collapsed on 15th November 2009 following heavy rains. A submerged bridge flow occurred in the Cedar River in Iowa after heavy rain in June 2008, which interrupted traffic on I-80. Dey and Barbhuiya (2004) reported the collapse of Bulls Bridge over the Rangitikei River, New Zealand. In another example by Bailey et al. (2002), "the Twin bridges on Interstate 5 over Arroyo Pasajero in California were destroyed during a flood, which resulted in the death of seven people." It must be mentioned that the failure of the New York State Thruway Bridge over Schoharie Creek on April 5, 1987, which cost 10 lives, has been attributed directly to local scour at bridge piers (LeBeau & Wadia-Fascetti, 2007). After this accident, the Federal Highway Administration required every state to monitor the situation of bridge scour.

Table 1.2 Summary of bridges damaged or destroyed by selected floods (David 2000)

Location	Number of Bridges Damaged or Destroyed
Calorado, 1965	63
South Dakota, 1972	106
Pennsylvania, West Virginia and Virginia, 1985	73
New York and New England, 1987	17
Midwest, 1993	>2,500
Georgia, 1994	>1,000
Virginia, 1995	74
California, 1995	45

The economic lost stemming from bridge failures is another important aspect. A sample of total highway damage repair costs caused by selected floods is given in Table1.3. Approximately 19 percent of federal-emergency funds used for highway restoration are allocated to bridge restoration (David 2000). In the period 1980-90, the Federal government spent an average of $20 million per year to fund bridge restoration projects (Rhodes and Trent, 1993). In New Zealand, scour related with floods results in the expenditure of NZ$36 million annually (Melville and Coleman, 2000). The report submitted to the DSIR (Department of Scientific and Industrial Research) of New Zealand indicated that 50 percent of the total expenditure of the DSIR was used for the bridges' restoration and maintenance (Macky, 1990) indeed 70 percent of the expenditures concentrated on bridge scour. Besides the direct expenditure for bridge scour, the indirect expenditure and the longer impact to the local economy merit our careful attention.

Table 1.3 Total highway damage repair cost for selected floods (David 2000)

Flood Location and Year	Repair Costs
Midwest - 1993	$178,000,000
Georgia - 1994	$130,000,000
Virginia - 1995	$40,000,000

Based on the harmfulness of the bridge scour discussed above, it deserves our attention and effort to solve it. Bridge scour problems are not only relevant to the existing bridges, but are also important to the safe design for new bridges. Many investigators pursued many years for better understanding of the scour mechanism, better scour

prediction methods and countermeasures against bridge scour (Alabi 2006). In spite of a lot of work, both the experimental and numerical studies, have been done to predict the behavior of the rivers and to quantify the equilibrium depth of scour, many researchers still are interested in the basic understanding of the scour mechanism. Based on the difference of the approach flow sediment transportation pattern, the local scour was divided into clear-water scour and live-bed scour (Chabert and Engeldinger, 1956).

Researchers put their efforts on various aspects of the bridge scour problem. Such as the local flow field around the abutment, the process of the scour, the parametric studies of scour and the scour depth change with time etc (Alabi 2006). As the practical meaning of the accurate prediction of the scour depth, most of the researches paid more attention on the study of the scour depth. More specifically, the study areas include the prediction of the scour depth in both uniform and nonuniform flow, the prediction of the scour depth on the condition of the free surface water or pressure water and the time scale for local scour etc. For example, Johnson and McCune (1991) developed an analytical model to simulate the temporal process of local scour at piers. Melville and Chiew (1999) presented an expression to enable the determination of the variation with time of scour at a pier.

Equilibrium scour is said to occur when the scour depth does not change with time. Equilibrium can also be defined as the asymptotic state of scour reached as the scouring rate becomes very small or insignificant (Patrick, 2006). Equilibrium scour depth under bridge-submerged flow at the clear water threshold condition has been studied by Arneson and Abt (1998), Umbrell et al. (1998), Lyn (2008), and Guo et al. (2009). These studies showed that equilibrium conditions are attained under very long

flow durations. According to Lyn (2008), even after 48 hours, an equilibrium scour depth could not be attained in his flume experiments. Guo et al. (2009) reported that for an approach flow depth of 25 cm, approach velocity of 0.4-0.5 m/s, sediment size of 1-2 mm, and bridge opening height of 10-22 cm, a time of about 42-48 hours was required for the scour depth to develop to its equilibrium value. If a model scale 1:40 and a Froude number similarity are used, these flow durations are equivalent to 11-13 days in prototype conditions, which may be much longer than the duration of a peak-flow in a flood event. In other words, the use of an equilibrium scour depth leads to overly conservative scour depth estimates that translate into excessive costs in the construction of bridge foundations. To improve the cost-efficiency of bridge foundation designs or retrofits, the time-dependent scour depth under bridge-submerged flow is of practical relevance.

The study of time-dependent scour depth has been reported extensively in literature for two decades, but all of them were, under free surface flow condition, about pier scour (Dargahi 1990, Yanmaz and Alitmbilek 1991, Melville 1992, Kothyari et al. 1992, Melville and Chiew 1999, Chang 2004, Oliveto and Hager 2005, Lopez et al. 2006, Yanmaz 2006, Lai et al. 2009) and abutment scour (Oliveto and Hager 2002, Coleman et al. 2003, Dey and Barbhuiya 2005, Yanmaz and Kose 2009). None of them were about general scour under bridge-submerged flow conditions (or pressurized flow conditions).

1.2 Objectives of Research

The objective of this study was to develop a semi-empirical model for computing the time-dependent variation of the maximum clear-water scour depth under bridge-

submerged flow. To this end, a series of flume tests was conducted to collect time-dependent scour data. A semi-empirical model was, next, developed based on the conservation of mass for sediment. The proposed model was, then, tested by the collected data. Finally, implications and limitations were noted for guiding practical applications and further research.

1.3 Synopsis of Thesis

In Chapter 2, the literature review about the basic knowledge of scour, the theoretical and experimental study about the prediction of the scour depth, the temporal development of scour and scour under bridge-submerged flow condition are covered. Chapter 3 gives a description of the experimental apparatus, models and procedures. Results and discussion of results are presented in Chapter 4. A Semi-empirical model for maximum scour depth is derived in Chapter 5. Finally, the main work of this study and recommendations for the future studies are presented in Chapter 6.

Chapter 2 Literature Review

2.1 Introduction

This chapter describes equipment and techniques used before this study to estimate scour depth at bridge piers and abutments. Most of the research results that are available for predicting the scour depth have been developed from small-scale, hydraulic modeling conducted in laboratories, and a limited amount of empirical data acquired from the field sites. Information about the previous studies was obtained mostly from the published papers. In order to familiarize the reader with terminologies germane to local scour and further understanding of scour. Some basic concepts about related with this study will be discussed briefly.

Although a vast literature exists relating to bridge scour, few reports deal specifically with the general scour under bridge-submerged flow condition (or pressurized flow condition). In the end of this section will talk about this point.

2.2 Scour

2.2.1 Definition of Scour

What is scour? Scour is the hole left behind when sediment (sand and rocks) is washed away from the bottom of a river. In order to provide more detail information, an advanced definition of bridge scour is often referred to “scour or erosion of the streambed and banks near the foundation (piers and abutments) of a bridge”. Breusers et al. (1977)

defined scour as a natural phenomenon caused by the flow of water in rivers and streams. It is the consequence of the erosion of flowing water, which removes and erodes material from the bed and banks of streams and also from the vicinity of bridge piers and abutments.

2.2.2 Types of Scour

Richardson and Davies (1995) claimed that the total scour at a river crossing can be divided into three components, including general scour, contraction scour and local scour.

It is acknowledged that under the interaction of the flow and sediment, the riverbed undergo the natural evolution in a long time. The unbalance of the scour and sediment is the root reason of the riverbed evolution. General scour is the removal of sediment from the river bottom by the flow of the river. The sediment removal and the resultant lowering of the river bottom is a natural process, but may remove huge amount of sediment over time. General scour is referred as degradation scour in some papers.

Contraction scour is the removal of sediment from the bottom and side of the river. It occurs when the natural flow area of a stream channel is reduced or constricted. Contraction scour is caused by an increase in speed of the water as it moves through a bridge opening that is narrower than natural river channel. The increase in velocity causes additional tractive shear stress on the bed surface, resulting in an increase in bed scour in the area of contraction (Umbrell et al. 1998).

Local scour is removal of sediment from around bridge piers or abutments. Piers are the pillars supporting a bridge. Abutments are the supports at each end of a bridge.

Water flowing past a pier or abutment may scoop out holes in the sediment; these holes are known as scour holes. As the local scour bring more damage to the bridges, researchers did a lot of work about this kind of scour. More phases about local scour will be discussed in the section of 2.3.

2.2.3 Areas Affected by Scour

Water normally flows faster around piers and abutments making them susceptible to local scour. At bridge openings, contraction scour can occur when water accelerates as it flows through an opening that is narrower than the channel upstream from the bridge. Degradation scour occurs both upstream and downstream from a bridge over large areas. Over long periods of time, this can result in lowering of the stream bed (http://en.wikipedia.org/wiki/Bridge_scour#cite_ref-presentation_1-1).

2.3 Local Scour

The basic mechanism causing local scour at piers is the formation of vortices (known as the horseshoe vortex) at their base (Figure 2.1).

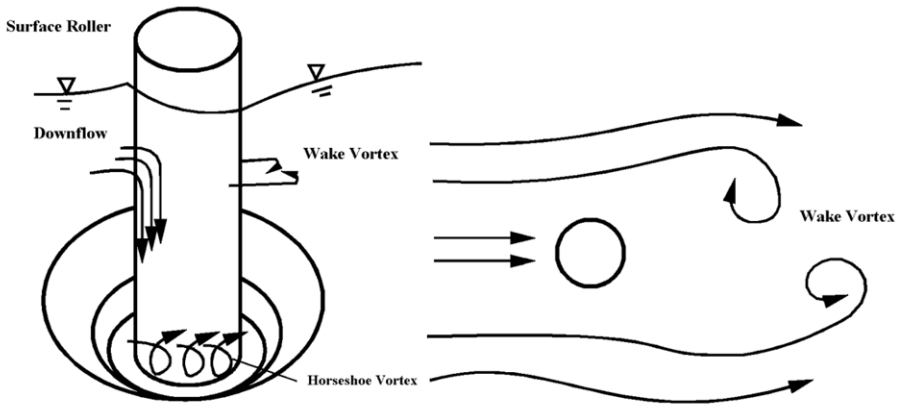

Figure 2.1 Illustration of the flow and scour pattern at a circular pier (Melville & Coleman 2000).

2.3.1 Flow Structure around the Bridge Pier

The flow structure at the vicinity of the bridge piers mainly include the decelerate flow before the pier, the stagnation pressure on the face of the pier and the vortex system around the piers. The strong vortex motion caused by the existence of the pier entrains bed sediments within the vicinity of the pier base (Lauchlan and Melville 2001). The down-flow rolls up as it continues to create a hole and, through interaction with the oncoming flow, develops into a complex vortex system. The vortex system is a kind of flow structure, and is the main considering factor in the predicting of the scour depth.

As illustrated in Figure 2.1, the pileup of water on the upstream surface of the obstruction and the acceleration of the flow around the nose of the pier or abutment lead a kind of vortex, named as horseshoe vortex because of its great similarity to a horseshoe (Breusers et al. 1977). In addition to the horseshoe vortex around the base of a pier, there are vertical vortices downstream of the pier called the wake vortex (Dargahi 1990). The horseshoe vortex caused the maximum velocity of the down flow more close to the piers. The wake vortex is the separation of the flow at the sides of the pier. Working like a vacuum machine, the lower pressure center makes the transport rate of sediment away from the base region is greater than the transport rate into the region, and consequently, a scour hole develops. Both the horseshoe and wake vortices remove material from the pier base region. However, the intensity of the wake vortices is drastically reduced with distance downstream. Therefore, immediately downstream of a long pier there is often deposition of material (Richardson and Davies, 1995).

2.3.2 Scour Depth and Velocity

When the approach flow velocity is smaller than the sediment entrainment velocity, the bed sediment keeps static. But under the effect of the vortex mentioned in the previous section, the local velocity near the bridge piers increased. Firstly, the upstream of the piers reached the entrainment velocity, the sediment started to move downstream and appeared the scour hole. If the scour hole is not refilled by the approach flow, named as the clear-water scour. Melville (1984) defined the clear water scour as the case where the bed sediment is not moved by the approach flow, or rather where sediment material is removed from the scour hole but not refilled by the approach flow. In contrast, the live-bed scour occurs when the scour hole is continually replenished with sediment by the approach flow (Dey 1999). Usually, the clear-water scour and live-bed scour consider as two classification of the local scour based on the pattern of sediment transportation.

View from the velocity relationship, the clear-water scour occurs for mean flow velocity up to the threshold velocity for bed sediment entrainment, i.e., u<= uc (Melville and Chiew 1999). On the other hand, live-bed scour occurs when u> uc. Melville and Raudkivi (1977), Chiew and Melville (1987) studied the influence to scour depth from the ratio of mean flow velocity and the threshold velocity for bed sediment entrainment. The conclusion is if the ratio is smaller than 0.5, no sour occurs; If the ratio is between 0.5 and 1, consider as clear-water scour; If the ratio is between 1 and 4, consider as the live-bed scour.

The time-dependent development of the scour depth under the clear-water and live-bed scour conditions is illustrated in Figure 2.2. From the Figure, the rapid development of scour depths under live-bed conditions (when sediment is generally in motion) means that the equilibrium scour depths are obtained rapidly for flow, but it fluctuates around the equilibrium scour depth. However, under clear-water conditions (the average approach flow V is less than the critical flow velocity for sediment entrainment), scour holes develop more slowly. An equilibrium clear-water scour depth is reached asymptotically with much longer time than live-bed condition. And the final equilibrium scour depth in clear-water scour is larger than that in live-bed scour.

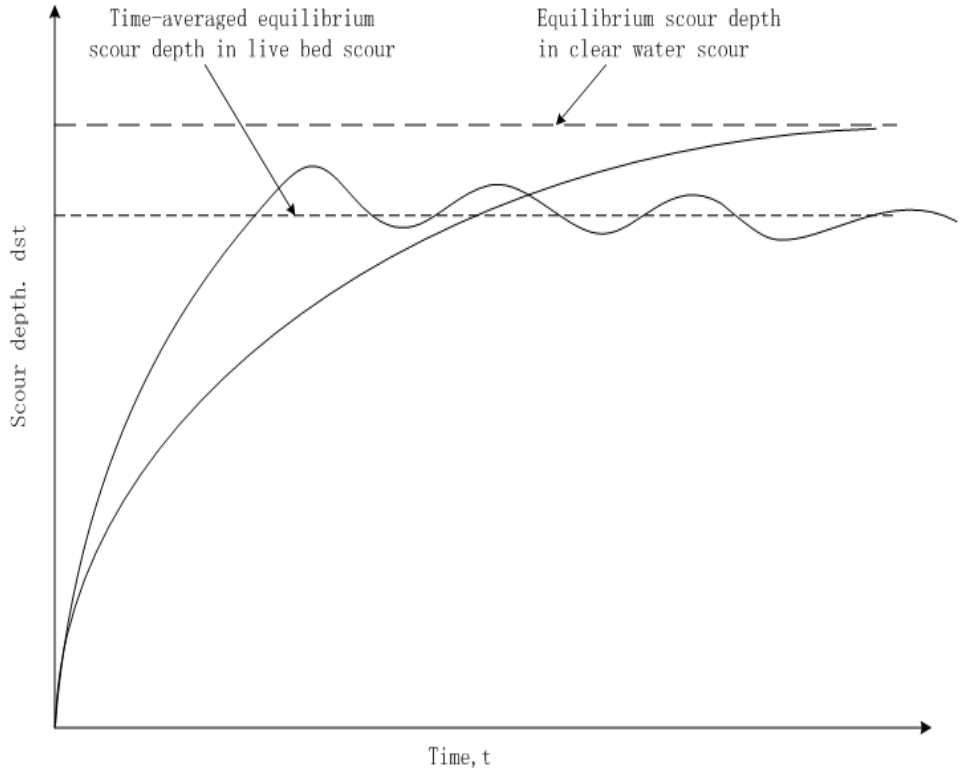

Figure 2.2 Time-dependent development of the scour depth (Raudlivi and Ettema 1983)

2.3.3 Local Scour Parameters

Assuming the flow is uniform steady flow, the factors that affect the magnitude of the local scour at piers and abutments can be grouped into four major headings.

1. Fluid parameters: flow intensity , kinematic viscosity and acceleration due to gravity ;
2. Approaching stream flow parameters: flow depth, Froude number, angle of attack of the approach flow to the pier;
3. Bed sediment parameters: sediment density, diameter of the sediment, grain size distribution, cohesiveness of the soil;
4. Pier parameters: size(i.e. the width of the pier), shape of the pier;

2.4 Local Scour Depth

To reduce the bridge failure caused by local scour and to improve the cost-efficiency of bridge foundation designs or retrofits, predict the local scour depth correctly is of practical relevance.

2.4.1 Equilibrium Scour Depth

As introduced previously, localized scour can occur as either clear-water scour or live-bed scour. The majority of the previous studies are devoted to determine the maximum depth of the scour around the bridge elements. Considering of the clear-water condition, the object of study is mostly based on estimation of the equilibrium depth of

the scour. The equilibrium scour depth is attained when the time-averaged transport of bed material into the scour hole equals that removed from it. The understanding of the equilibrium scour depth varies from different researchers. Anderson (1963) states "By virtue of the logarithmic character of the development of the scour region with time, a practical equilibrium is reached after a relatively short time, after which the increase in the depth and extent of scour becomes virtually imperceptible". However, Rouse (1965) claims that scour is an ever-increasing phenomenon and there is no real equilibrium scour depth. This opinion was agreed by Bresuers (1963, 1967) and Kohli and Hager (2001). But more investigators believe that an equilibrium scour depth does exist (Laursen 1952, Carstens 1966, Gill 1972) and gave the definition of it. Franzetti et al. (1982) refer to equilibrium as the state of scour development where no further change occurs with time. Equilibrium can also be defined as the asymptotic state of scour reached as the scouring rate becomes small or insignificant (Patrick 2006).

The equilibrium scour depth is subject to influence of flow and sediment parameters. In the related literature, equilibrium scour depth is written as a function of the velocity, flow depth and particle size. For a given pier, sediment, and approach flow velocity and the concomitant estimation of the scour depth at any stage during the development of the equilibrium scour hole, the method was given for getting the equilibrium scour depth (Melville and Chiew, 1999).

2.4.2 Temporal Variation of Scour

In order to enlighten the mechanisms responsible for the scouring phenomenon, several aspects are need to be clarified, one of them is the temporal variation of scour.

Local scour around the bridge elements is a time dependent phenomenon. It is always represented in graphic form by plotting the maximum scour depth against the time. It is difficult to get the accurate maximum scour depth in a given time due to the complexity of the scour process. Therefore, many methods have always been considered to yield the relationship of the maximum equilibrium scour depth and time.

Attempts to describe the temporal development of scour have been made by various authors in the past half century, as shown is Table 2.1. Among of them, Melville and Chiew (1999) did a lot of significant work. They claimed that the temporal development of scour is dependent on the condition of flow, geometry and sediment parameters based on the data from about 35 experiments that covered a wide range of pier diameter, flow depth and approach floe velocity. The significant conclusions are the scour depth after 10% of the time to equilibrium is between about 50% and 80% of the equilibrium scour depth. And for a given approach flow depth and velocity ratio, the time to equilibrium increases with increasing pier diameter.

Table 2.1 The study of the temporal development of scour

Year	Investigator(s)	Work	Special
1956	Chabert and Engeldinger	introducing the effects of time and velocity on clear water and live bed local scouring at bridge piers	first
1965	Shen et al.	studied time-dependent variation in clear water scouring around bridge piers	

1980	Ettema	performed an experimental study on temporal variation of scour around piers in uniform, non-uniform and layered bed sediments	non-uniform
1983	Raudkivi and Ettema	developed a chart giving temporal variation in scour depth around cylindrical piers using non-uniform sediments	non-uniform
1991	Yanmaz and Altmbilek	introduced a semi-empirical model giving time-dependent variation in clear water scour depth around cylindrical and square piers in uniform bed material	semi-empirical model
1992	Kothyari et al.	studied the temporal variation of scour depth at bridge piers under clear-water scour condition with unsteady flow	unsteady flow
1994	Chatterjee et al.	measured the time variation of scour depth downstream of an apron due to a submerged jet	
1999	Melville and Chiew	developed an empirical equation giving the temporal variation in clear water scour at cylindrical bridge piers in uniform sediments as a function of equilibrium scouring parameters.	empirical equation for equilibrium conditions

2002	Oliveto and Hager	gave temporal variation in clear water scour depth around piers in non-uniform sediments	non-uniform
2004	Chang et al.	carried out experiments under steady and unsteady water condition, with uniform and non-uniform sediment to predict the evolution of scour depth	steady and unsteady, uniform and non-uniform
2005	Dey and Barbhuiya	developed a semi-empirical model to compute the temporal variation of scour depth for short abutment	short abutment

2.4.3 Equations for Describing Temporal Variation of Scour

A study of US Federal Highway Administration in 1973 concluded that of 383 bridge failures, 25% involved pier damage and 72% involved abutment damage (Richardson et al 1993). So many investigators focused on giving the equation for describing temporal variation of scour based on the local scour at piers and abutments.

Rouse (1965), Gill (1972), Rajaratnam and Nwachukwu (1983), Dargahi (1990), Ettema (1980), Kohli and Hager (2001), Oliveto and Hager (2002) and Coleman et al (2003) think that the variation of scour depth with time is logarithmic.

Kohli and Hager (2001) conducted laboratory experiment to study the influence of test duration on the scour depth at vertical –wall abutments placed in floodplain. They

found that densimetric particle Froude number has a significant effect on the scour depth. They gave a logarithmic function of time-variation of scour depth as

$$d_{st} = (F_d^2/10)(hl/\cos\theta_a)^{0.5} log[t(\Delta g d)^{0.5}/10h] \quad (2.1)$$

in which F_d is the densimetric Froude number, h is the approaching flow depth, l is the transverse length or protrusion length of abutment, θ_α is angle of attack , d is the median diameter of sediment particles.

In the published paper, Oliveto and Hager presented new research on bridge pier and abutment scour based on a large data set collected at ETH Zurich, Switzerland. In total six different sediments were tested, of which three were uniform. An equation for temporal scour evolution was proposed and verified with the available literature data. The limitations relating to hydraulic, granulometric, and geometrical parameters are excluded in the scour equation as follows:

$$d_{st}/L_R = 0.068 N_s {\sigma_g}^{-1/2} F_d^{1.5} \log(T_R) \qquad F_d > F_{di} \quad (2.2)$$

which L_R is the reference length $l^{2/3}h^{1/3}$, N_s is the shape number, σ_g is the geometric standard deviation, T_R is the dimensionless time, N as a shape number equal to N = 1 for the circular pier, and N =1.25 for the rectangular abutment (or pier). The sediment standard deviation σ has a definite effect on scour and was recently established for inception of sediment transport.

Coleman et al (2003) analyzed the time-variation of scour depth at vertical-wall abutment under clear-water condition. They put forward the following equation:

$$d_{st}/d_s = exp[-0.07(U_C/U)|ln(t/T)|^{1.5}] \quad (2.3)$$

Ahmad (1953), Franzetti et al (1982), Kandasamy (1989), Whitehouse (1997), Caedoso and Bettess (1999) and Ballio and Orsi (2000) propose an exponential time-variation of scour; while Bresuers (1967) and Cunha (1975) give a power law distribution.

Franzetti et al. (1982) studied the influence of test duration on the ultimate scour depth at a circular pier and suggested an exponential of the form

$$y_s = y_{se}\left(1 - exp(-BT^C)\right) \tag{2.4}$$

$$T = \frac{ut}{D} \tag{2.5}$$

where y_s = scour depth; y_{se} = ultimate or equilibrium scour depth; B and C are constants; T = dimensionless time; u = mean velocity of the approach flow; t = time; and D = pier diameter. After conducting a series of experiments, Franzetti et al. got the number range of B and C, they adopted the average value of these constants. The equation finally becomes

$$y_s = y_{se}\left(1 - exp\left(-0.028T^{1/3}\right)\right) \tag{2.6}$$

Cunha (1975) gave an expression of the form $y_s = KT^C$, where K has the unit of length, C is a dimensionless constant and T is the dimensionless time.

In the following study, Simarro-Grande and Martin-Vide compared the Cunha (1975) expression with that of Franzetti et al. (1982), and found that the value of K can be approximated as $K = y_{se}B$ and also observed that the value of C is approximately equal for each equation. Another important equation was posed by Melville and Chiew (1999), based on series of experiments for pier scourge under clear-water conditions, they presented in the paper:

$$y_s/y_{se} = exp\left(-0.03\left|\frac{u_c}{u}\ln(\frac{t}{t_e})\right|^{1.6}\right) \tag{2.7}$$

$$T^* = \frac{ut_e}{D} \tag{2.8}$$

$$T^* = 1.6 * 10^6 \left(\frac{y_0}{D}\right)^{0.25} \qquad for \quad \frac{y_0}{D} \leq 6 \tag{2.9}$$

$$T^* = 2.5 * 10^6 \qquad for \quad \frac{y_0}{D} > 6 \tag{2.10}$$

where T* is the dimensionless equilibrium time scale and t_e represents the time to the equilibrium scour condition. The critical velocity u_c which is dependent on the flow depth, was determine using the semi-logarithmic average velocity equation for a rough bed.

2.4.4 Estimation of Equilibrium Scour Depth

Estimation of the equilibrium scour depth is needed for economical and secure design of the infrastructural components of bridges. While underestimation of the scour depth leads to the design of too shallow a bridge foundation, on the other hand, overestimation leads to uneconomic design on the other (Ting et al. 2001). A majority of the scour studies have been carried out for giving the equilibrium scour depth prediction equation.

Although it is claimed that during a flood event the maximum scour depth at peak-flow may be much smaller than the equilibrium scour depth, there are few investigations for estimating the maximum scour depth under real flood flow. Instead of this, the design flow condition is chosen for prediction of the equilibrium scour depth.

Most of the equilibrium scour depth predicting equations are empirical equations. Both the experimental laboratory data and field data are essential in deriving these equations. A number of studies have been carried out with a view to determining the

equilibrium scour depth for clear water scour under steady flow condition. Such as Laursen (1958), Neill(1964), Shen et al.(1969), Breusers (1977), Raudkivi and Ettema (1983), Yanmaz and Altinbilek (1991) and Melville and Chiew (1999).

Based on the Laursen and Toch (1956) data, Breusers et al. (1977) presented an equation to calculate the equilibrium scour depth:

$$y_{se} = 1.35K_i b^{0.7} y_0^{0.3} \tag{2.11}$$

where K_i=1.0 for circular pier, b = pier width, y_0 = flow depth.

Colorado State University gave an equation involved the Froude number to predict the equilibrium scour depth, the prediction equation is as follows:

$$y_{se} = 2.0K_i y_0 F_r^{0.43} \left(\frac{b}{y_0}\right)^{0.65} \tag{2.12}$$

where Ki =1.1 for a circular pier with clear-water scour, Fr is Froude number.

2.5 Scour Under Bridge-Submerged Flow Condition

The studies of bridge scour usually assume an un-submerged bridge flow, but the flow regime can switch to submerged flow when the downstream edge of bridge deck is partially or totally inundated during large flood events. Figure 2.3 shows a bridge undergoing partially submerged flow in Salt Creek, NE, in June 2008. More an example, a submerged bridge flow occurred in the Cedar River in Iowa after rain in June 2008 (Figure 2.4), which interrupted traffic on I -80. Submerged flow most likely creates a severe scouring capability because to pass a given discharge, the flow under a bridge can only scour the channel bed to dissipate its energy.

Figure 2.3 Fhoto. Partially inundated bridge deck at Salt Creek, NE

Figure 2.4 Submerged-flow of Cedar River bridge on I-80 in Iowa in June 2008

Review the aforementioned studies, only Arneson and Abt (1998), Umbrell et al. (1998) and Lyn (2008) investigated on the submerged-flow bridge scour. Arneson and Abt (1998) in Colorado State did series of flume tests and proposed the following regression equation.

$$\frac{y_s}{h_u} = -0.93 + 0.23\left(\frac{h_u}{h_b}\right) + 0.82\left(\frac{y_s+h_b}{h_u}\right) + 0.03\left(\frac{V_b}{V_{uc}}\right) \quad (2.13)$$

where ys = maximum equilibrium scour depth, hu = depth of approach flow before scour, h_b= vertical bridge opening height before scour, V_b = velocity through a bridge before scour, and V_{uc} = upstream critical approach velocity defined by

$$V_{uc} = 1.52\sqrt{g(s-1)d_{50}}\left(\frac{h_u}{d_{50}}\right)^{1/6} \quad (2.14)$$

where g = gravitational acceleration, s = specific gravity of sediment, and d_{50} = median diameter of bed materials. Although Eq. (2.13) has been adopted in the FHWA manual (Richardson and Davis 2001), it suffers from a spurious correlation where both sides of the equation include y_s/h_u. In the meanwhile, Umbrell et al. (1998) also conducted a series of flume tests in the FHWA J. Sterling Jones Hydraulics Laboratory. Using the mass conservation law and assuming that the velocity under a bridge at scour equilibrium is equal to the critical velocity of the upstream flow, they presented the following equation

$$\frac{y_s+h_b}{h_u} = \frac{V_u}{V_{uc}}\left(1-\frac{b}{h_u}\right) \quad (2.15)$$

where V_u = approach flow velocity that is less than or equal to the critical velocity V_{uc}, and b = thickness of the bridge deck. By comparing Eq. (2.15) with their flume data, Umbrell et al. modified Eq. (2.15) as follows

$$\frac{y_s+h_b}{h_u} = 1.102\left[\frac{V_u}{V_{uc}}\left(1-\frac{b}{h_u}\right)\right]^{0.603} \quad (2.16)$$

where the critical velocity is estimated by Eq. (2.14) except that the coefficient, 1.52, is replaced by 1.58. Eq. (2.15) or (2.16) was based on the mass conservation law, but the dynamic law of momentum or energy was overlooked, which weakens the foundation of predictions because scour is a dynamic process. Besides, Umbrell's tests were run only for 3.5 hours that is not enough time for equilibrium scour to develop although they

extrapolated their results to equilibrium states. The latest study was reported by Lyn (2008), who reanalyzed Arneson's and Umbrell's data sets and proposed the following power law

$$\frac{y_s}{h_u} = min\left[0.105\left(\frac{V_b}{V_{uc}}\right)^{2.95}, 0.5\right] \quad (2.17)$$

where V_b and V_{uc} are the same as in Eq. (2.13). Lyn's equation is an empirical model, but he identified the spurious regression of Eq. (2.13) and the low quality of Umbrell's data set.

Recently, Guo et al. (2009) divided bridge – submerged flow into three cases. They are as follows:

Case 1

If the downstream low chord of a bridge is un-submerged as shown in Figure 2.5, the bridge operates as an inlet control sluice gate. The scour is independent of the bridge width and continues until a uniform flow and a critical bed shear stress are reached. This case occurs only for upstream slightly submerged conditions.

Case 2

If the downstream low chord is partially submerged as shown in Figure 2.6, the bridge operates as an outlet control orifice, and the bridge flow is rapidly varied pressure flow.

Case 3

If the bridge is totally submerged as shown in Figure 2.7, it operates as a combination of an orifice and a weir. Only the discharge through the bridge affects scour depth. In this study, the experimental condition as case 3.

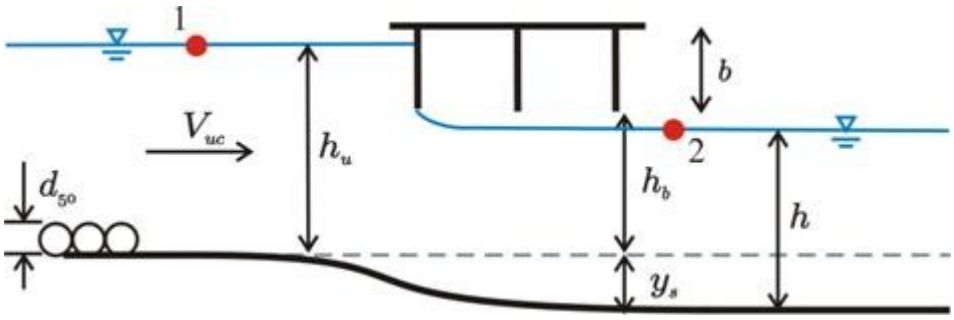

Figure 2.5 Illustration pressure flow for case 1

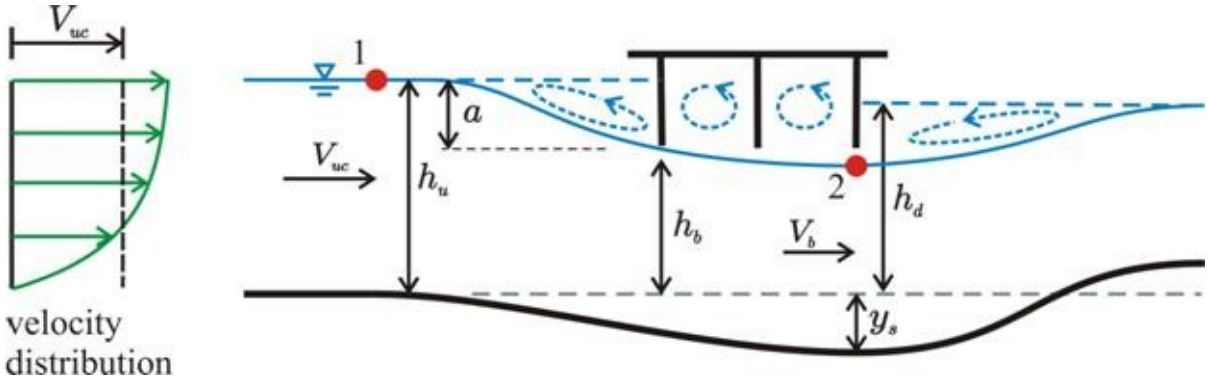

Figure 2.6 Illustration pressure flow for case 2

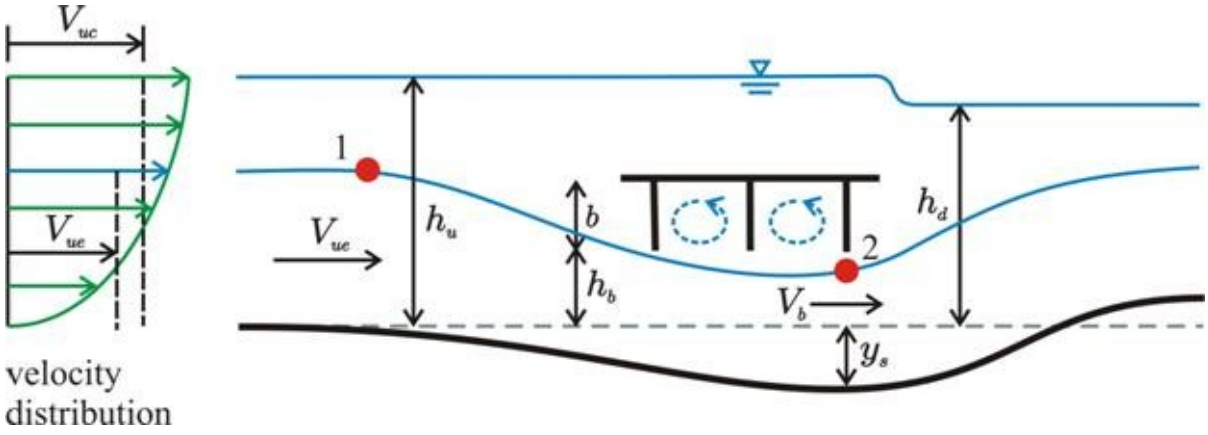

Figure 2.7 Illustration pressure flow for case 3

According to Guo et al. (2009), scour of case 1 can be estimated by the traditional critical shear stress or critical velocity method. Scour of case 2 and case 3 can be estimated by the following equations:

$$\frac{h_b + y_s}{h_b + a} = \sqrt{\frac{1 + \frac{\lambda}{F^m}}{1 + \frac{2\beta}{F^2}}} \tag{2.18}$$

or

$$\frac{h_b + y_s}{h_b + b} = \sqrt{\frac{1 + \lambda\left[\frac{g(h_u - h_b)}{V_{ue}^2}\right]^{m/2}}{1 + \frac{2g(h_u - h_b)}{V_{ue}^2}}} \tag{2.19}$$

where hb is the bridge opening, ys is the maximum scour depth, a is the deck block depth, b is the thickness of bridge deck including girders, λ is an empirical fitting factor, F is inundation Froude number, m is fitting parameter in the bridge energy loss coefficient, β is the correction factor for hydrostatic pressure under bridge, hu is the depth of headwater, Vue is the upstream effective velocity.

In the following chapters we will emphasize on the time-dependent scour of bridge-submerged flow.

Chapter 3 Experimental Setup and Methodology

3.1 Introduction

In this chapter, the experimental arrangements, hydraulic models, data acquisition system and variables measured in the model study are described. The experimental study was aimed at understanding the time-dependent scour processes in bridge-submerged flow and collecting data for the development of a semi-empirical model for scour depth. All of the experiments were conducted by Dr.Lianjun Zhao in the FHWA J. Sterling Jones Hydraulics Laboratory, located at the Turner-Fairbank Highway Research Center in McLean, VA.

3.2 Flume

The experiment in this study was conducted in a circulating flume. The flume had a length of 21.35 m, width of 1.83m, and depth of 0.55 m with clear sides and a stainless steel bottom whose slope was 0.0007%. In the middle of the flume was installed a working section in the form of a recess, which is filled with sediment to a uniform thickness of 0.4 m. The sand bed recess is 3.04 m long and 0.63 m wide with a model bridge above it. A honeycomb flow straightener and a trumpet-shaped inlet were carefully designed to smoothly guide the flow into the working channel. The circulating flow system is served by a pump with capacity of 0.3 m^3/s, located at the downstream end

of the flume. The pump takes the water from a sump at the downstream end of the flume. The sump, which is 210 m^3 located immediately at the downstream of the flume and separated from it by a tailgate. The depth of flow was also controlled by the tailgate. The water discharge was measured by a LabView program and checked by an electromagnetic flow meter. Figure 3.1 shows a schematic illustration of the experimental flume system. Figure 3.2 shows a photograph of the experimental model.

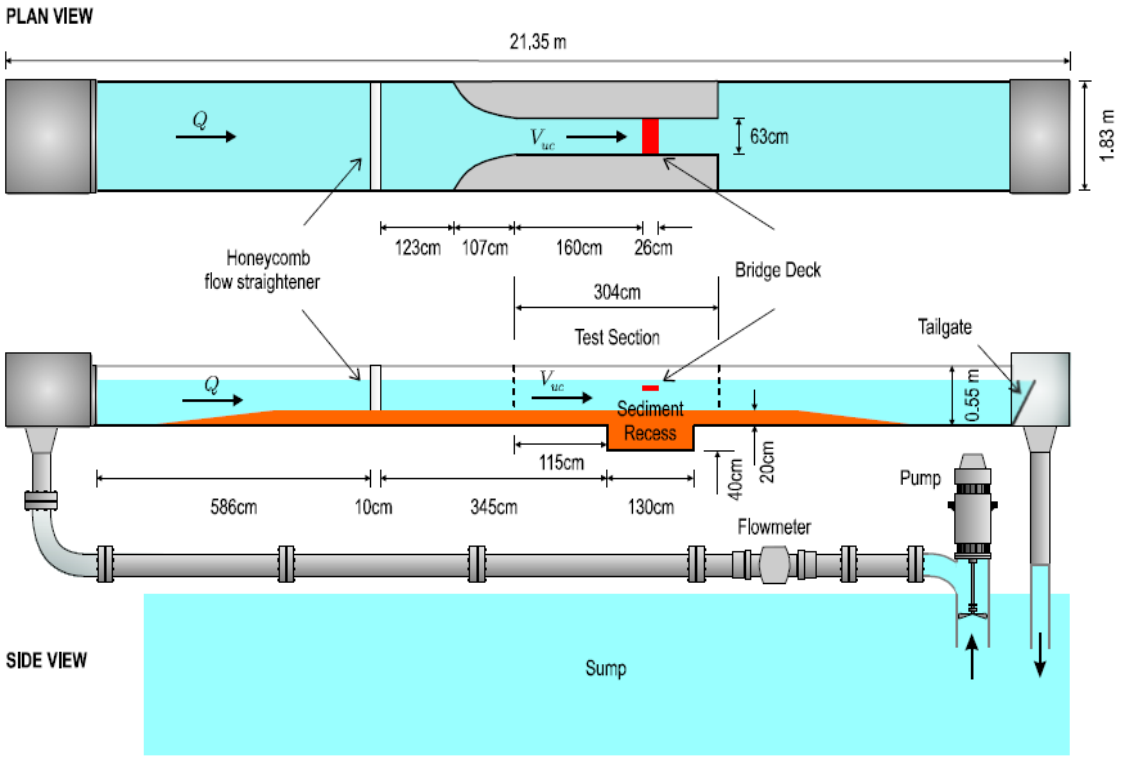

Figure 3.1 Schematic illustration of the experimental flume system

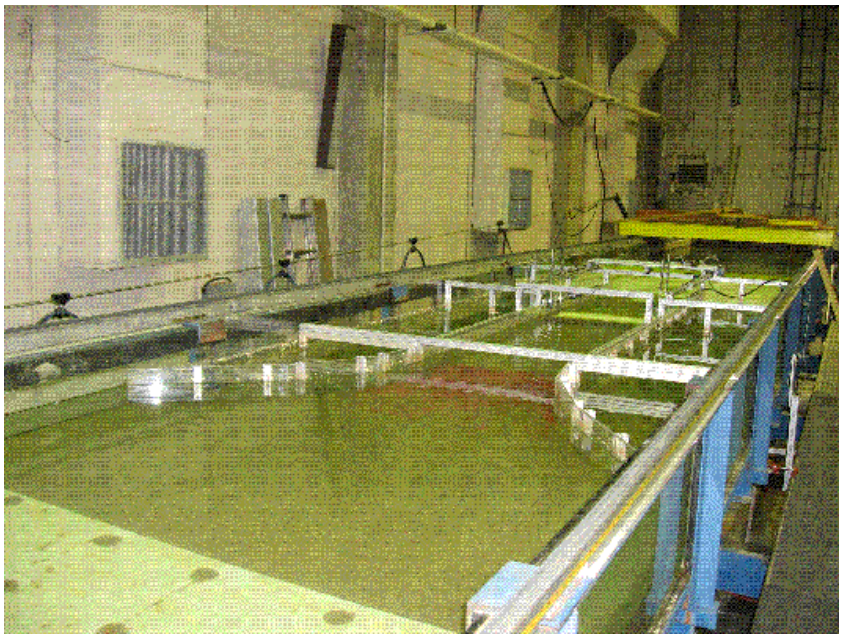

Figure 3.2 Photographs of the experimental model

3.3 Flow Conditions

A LabView program was used to control an automated flume carriage that was equipped with a Micro Acoustic Doppler Velocimeter (MicroADV) for records of velocities and a laser distance sensor for records of depths of flow and scour. Acoustic Doppler Velocimeters are capable of reporting accurate mean values of water velocity in three directions (Kraus et al., 1994; Lohrman et al., 1994; Voulgaris et al., 1998) even in low flow conditions (Lohrman et al., 1994). The SonTek MicroADV is a versatile, high-precision instrument used to measure 3D water velocity. The MicroADV is used to measure water velocity in a wide range of environments including laboratories, rivers, estuaries and the ocean. An ADV measures three-dimensional flow velocities using the Doppler shift principle and consists, basically, of a sound emitter, three sound receivers

and a signal conditioning electronic module. The emitter of the instrument generates an acoustic signal that is reflected back by sound-scattering particles present in the water (assumed to move at the water velocity). This scattered sound signal is detected by the instrument receivers and used to compute the signal Doppler phase shift with which the radial flow velocity component is calculated. The MicroADV (SonTek 1997) measures 3-dimensional flow in a cylindrical sampling volume of 4.5 mm in diameter and 5.6 mm in height with a small sampling volume located about 5 cm from the probe; with no zero offset, the MicroADV can measure flow velocities from less than 1 mm/s to over 2.5 m/s. The velocity profile measuring device MicroADV(SonTek 1997) is shown in Figure 3.3.

Figure 3.3 MicroADV(SonTek 1997)

In the present experiments, velocity measurements were taken in a horizontal plane located at a cross-section 22 cm upstream of the bridge. The LabView program was set to read the MicroADV probe and the laser distance sensor for 60 seconds at a scan rate of 25 Hz. According to the instructions, the MicroADV has an accuracy of ±1% of measured velocity, and the laser distance sensor has an accuracy of ±0.2 mm.

This study emphasizes clear water scour since it is usually larger than the corresponding live bed scour. To ensure a clear water scour under the bridge, the approach velocity in the test channel must be less than the critical velocity, which can be preliminarily calculated by Neill's (1973) equation and adjusted by a trial-and-error method. Since the flow depths in the experiments were always kept at 25 cm, according the equation

$$V_C = 1.52\sqrt{g(s-1)d_{50}}\left(\frac{h_u}{d_{50}}\right)^{1/6} \tag{3.1}$$

where g = gravitational acceleration, s = specific gravity of sediment, and d_{50} = media diameter of the bed materials. The critical velocity is about

$$Vc = 0.485 \text{ m/s}$$

which corresponds to a maximum allowable discharge in the test channel.

$$Qmax = (0.485 \text{ m/s})\ (0.63 \text{ m})\ (0.25 \text{ m}) = 0.0764 \text{ m}^3/\text{s}$$

Based on the calculation above, two discharges were applied in the experiments. They were determined by a critical velocity and the flow cross-section in the test channel that had a width of 0.63 m and a constant flow depth of 0.25 m. The critical velocity of sediment $d_{50} = 1.14$ mm was approximately 0.425 m/s and the corresponding experimental discharge Q was 0.0669 m^3/s. The critical velocity of sediment $d_{50} = 2.18$ mm was approximately 0.482 m/s, and the corresponding experimental discharge was 0.0759 m^3/s.

3.4 Sand Bed

Figure 3.4 shows the sand bed preparation in the test channel. To test the effect of sediment size on scour morphology, two uniform sands (the gradation coefficient

$\sigma_g < 1.5$) were used: a median diameter $d_{50} = 1.14$ mm with $\sigma_g = 1.45$, and a median diameter $d_{50} = 2.18$ mm with $\sigma_g = 1.35$.

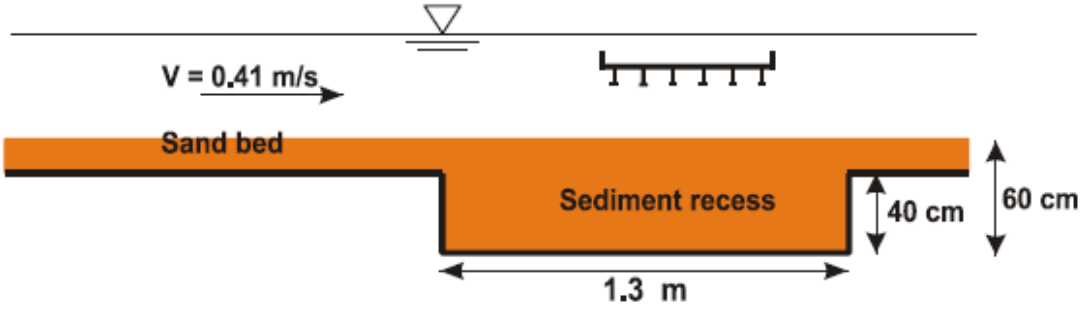

Figure 3.4 Sand bed preparation in the test section

3.5 Model

A previous study (Guo et al. 2009) has shown that the scour depth in submerged flow is independent of the number of girders so that only a six-girder deck was tested in the present study. The six-girder deck, made of special Plexiglas (shown in the Figure 3.5), was chosen since most four lane US highway bridges have six girders. The deck has rails at the edges that allow water to pass through onto the deck surface. The deck elevation was adjustable, permitting the deck to have eight different inundation levels.

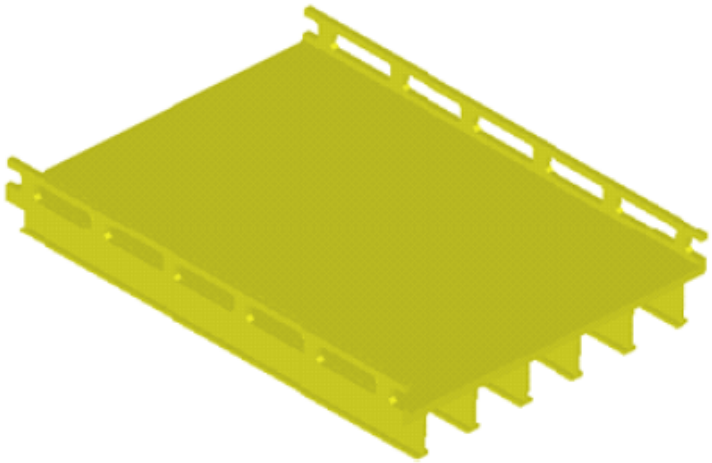

(a) 3D view of the 6-girder deck

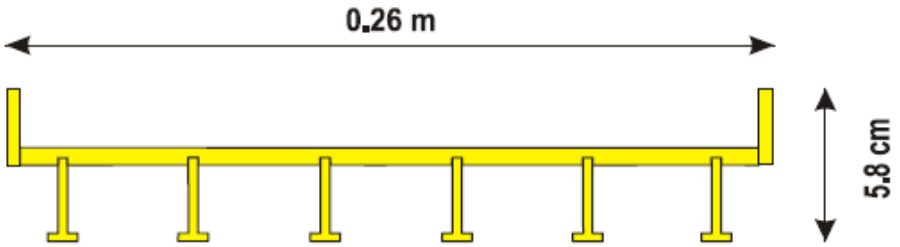

(b) Cross-section of the 6-girder deck

Figure 3.5 Model deck of the experiment

3.6 Statement of the Problem and the Experiment Conditions

The experimental setup is shown in Figure 3.6: Without contraction channel and piers, a bridge crossing over a river clear water flow, where Vu = velocity of the upstream flow, B = width of the river, W = width of the bridge deck, d_{50} = median diameter of the bed materials, h_u = depth of the upstream flow, h_b = bridge opening before the scour, b = thickness of the bridge deck, and y_s = maximum scour depth. Determine the maximum scour depth y_s in Figure 3.6 by considering a unit river flow.

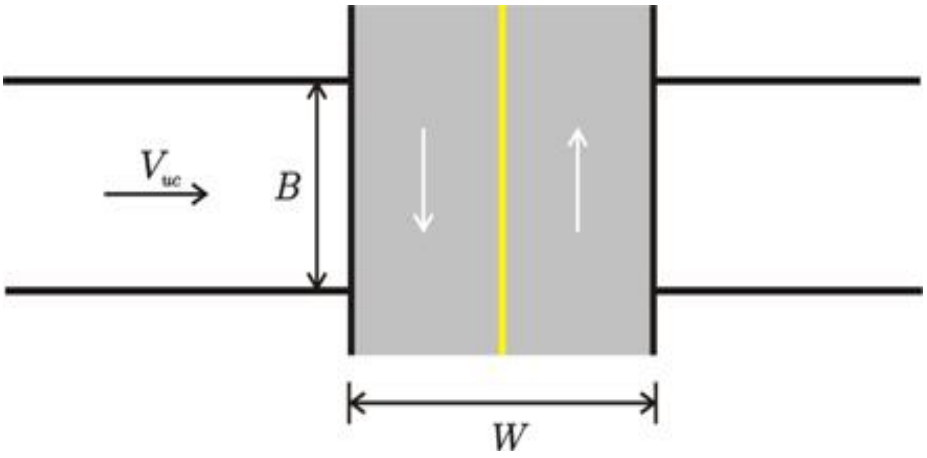

(a) Plan of a bridge crossing

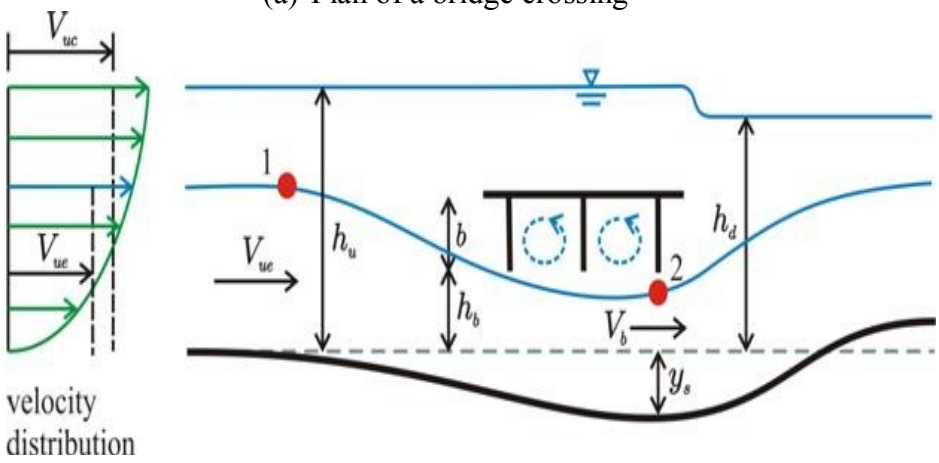

(b) Centerline cross-section

Figure 3.6 Flow through bridge without contraction channel and piers

To study the scour processes, scour morphologies at eleven times were measured for each given bridge opening height. The settings of the flow, sediment, bridge height and designated times are listed in Table 3.1, where the Froude and Reynolds numbers show that the approach flows were subcritical turbulent flows.

Table 3.1 Experimental conditions

Approach flow conditions:	$h_u = 25\,\text{cm}$, $R_h = 13.9\,\text{cm}$, $V_u = 42.5\,\text{cm/s}$ for $d_{50} = 1.14\,\text{mm}$ with $\sigma_g = 1.45$, $\text{Re} = 59100$, Fr= 0.271 $V_u = 48.2\,\text{cm/s}$ for $d_{50} = 2.18\,\text{mm}$ with $\sigma_g = 1.35$, $\text{Re} = 66700$, Fr=0.308
Bridge opening heights:	$h_b = 13, 16,$ and 19 cm
Scour measurements at:	t=0.5,1,2,4,8,12,16,20,24,30,36 and 42 hours

Note: R_e is based on hydraulic radius, and Fr based on flow depth.

3.7 General Experimental Procedure and Data Acquisition

For each test with designated bright height and scour time, the experimental procedure as follows: 1) Filled the sediment recess with sand and evenly distributed sand on the bottom of the flume until the depth of sand was 60 cm in the sediment recess and 20 cm in the test channel. 2) Installed a bridge deck at a designated elevation and positioned it perpendicular to the direction of flow. 3) Pumped water gradually from the sump to the flume to the experimental discharge that was controlled by the LabView. 4) Checked the approach velocity distributions in the vertical and lateral to see if they were more or less uniform away from the walls, and ran each test until the designated time. 5) Gradually emptied water and carefully removed the model bridge from the flume. 6) Scanned the 3-dimensional scour morphology using the laser distance sensor with a grid size of $5\,\text{cm} \times 5\,\text{cm}$.

An automated flume carriage fitted to the main flume, shown in Fig.3.7, was used to collect data of velocity field and scour depths. The scour depths were measured using a laser distance sensor while the velocity field was measyred using a PIV system. A Lab

VIEW program was applied for data acquisition, instrument control, data analysis, and report generation.

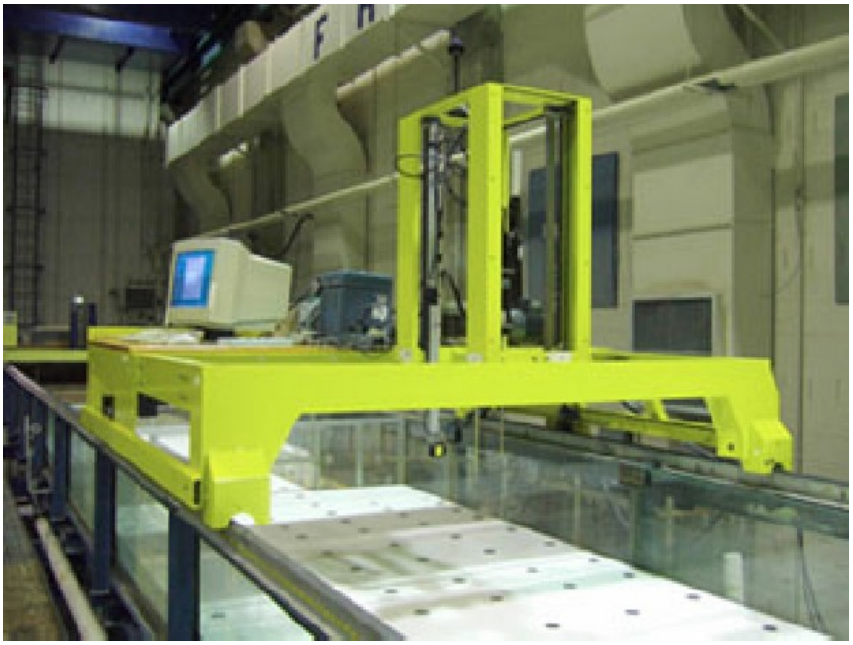

Figure 3.7 The automated flume carriage fitted to the main flume

Chapter 4 Results and Discussion

4.1 Introduction

The objective of this study was to present a design method for time-dependent scour depth under bridge-submerged flow. A series of flume experiments on scour depth under bridge-submerged flow were carried out to collect scour data at different times. In this chapter, the results obtained from all of the experiments are presented. The analyses and the discussion of the results are presented subsequently. The experimental results include the velocity distributions of the approach flow, the records of 3-dimensional scour morphology, the width-averaged 2-dimensional longitudinal scour profiles, and the width-averaged maximum scour depths.

4.2 Velocity Distribution

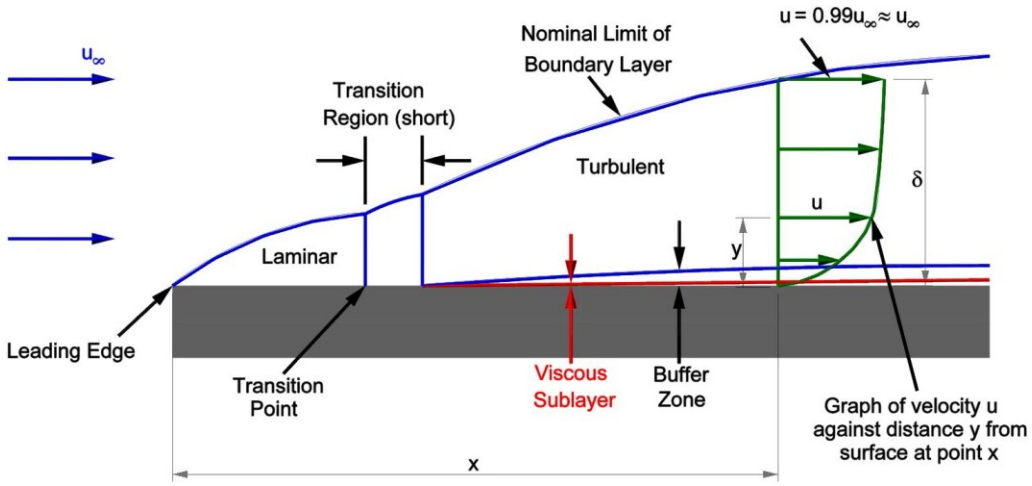

Figure 4.1 Boundary layer on a flat plate

Source: http://www.cortana.com/20061218_Boundary_Layer_of_Flat_Plate_jpg.jpg

As indicated by figure 4.1, which shows the development of boundary length as the flow passes over a solid surface, flow along the flume encounters resistance which is proportional to the roughness of bounding walls with the development of boundary layers. Boundary layers appear on the surface of bodies in viscous flow because the fluid seems to "stick" to the surface. When a fluid flows over a stationary surface, e.g., the bed of a river or the wall of a pipe, the fluid touching the surface is brought to rest by the shear stress at the wall. The velocity increases from the wall to a maximum in the main stream of the flow. The boundary layer thickness will increase with distance from the point where the fluid first starts to pass over the boundary. It increases to a maximum in fully developed flow. Correspondingly, the friction on the fluid due to shear stress to at the wall increases from zero at the start of the plate to a maximum in the fully developed flow region where it remains constant.

At the entrance to the flume a high-velocity gradient is developed in the vicinity of the flume bed, which is associated with the frictional stresses generated between the fluid particles and the sand. A boundary layer is developed adjacent to the sand bed, which may be laminar (i.e. a constant motion within layers) at the upstream end due to viscous shear stress (as shown in figure 4.1), steadily thickens to a certain point in the flume length in which the flow is called developing flow. Beyond this location it becomes fully developed flow, and the boundary layer might become turbulent due to incapability of the shear stress to hold the flow in layers. Since the velocity profiles of a developing and developed flow are different, the characteristics of the approaching flow can be revealed by investigating the velocity distribution of flow before the bridge.

In this study, the velocity distributions in the approach flow were measured in the first half hours, which showed nearly uniform velocity distribution flow over a cross-section because the bottom and sidewall boundary layers were not fully developed. Two representative measured velocity distributions over a cross-section located at 22 cm upstream of the bridge are shown in Fig.4.2 where both the flow depths were 25 cm, the average velocity for d_{50} = 1.14 mm was 0.41 m/s and the average velocity for d_{50} = 2.18 mm was 0.53 m/s. Fig.4.2 (a) shows five vertical velocity distributions over the cross-section for two different tests where data near the bottom ($y < 5$ cm) and near the free surface ($y > 17$ cm) could not be accurately measured due to the distance requirements for the probe, according to SonTek (1997). Fig.4.2 (b) shows the corresponding depth-averaged velocity distributions along the lateral where data near the side walls were not measured due to the same reason. The near wall velocity distributions were extrapolated by a 1-7th power law for explanation.

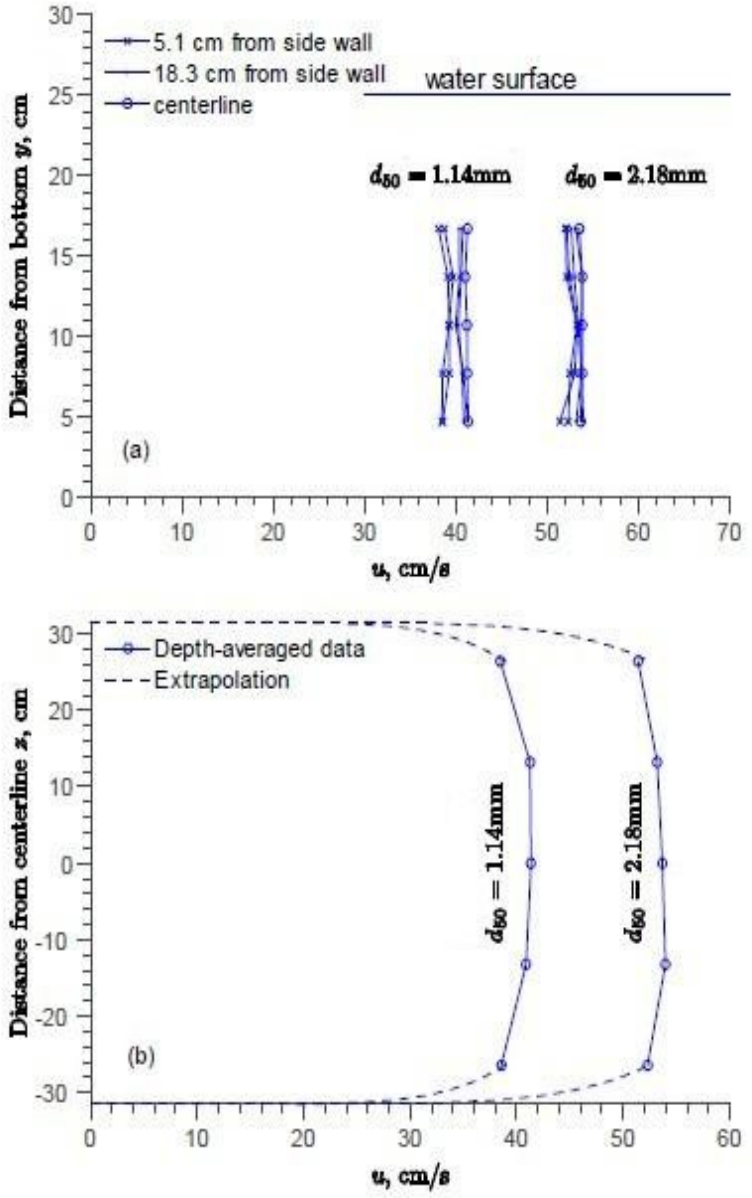

Figure 4.2 Velocity distribution of approach flow (a) vertical distribution, and (b) lateral distribution

Figure 4.2(a) shows that the velocity distribution for each vertical is approximately a constant, which implies that the bottom boundary layer upstream of the bridge was not fully developed, and the boundary layer thickness was less than or equal

to 5 cm. Similarly, the depth averaged velocity distribution in the lateral for each test in the center of the flume (where -15 cm< z <15 cm), shown in Figure 4.2(b), is also nearly a constant, which means the two side wall boundary layers were not fully developed, either. These undeveloped boundary layers resulted from the short length of the test section upstream of the bridge. They affect the bridge flow in two ways: friction upstream of the bridge and flowrate through the bridge. Since bridge flows are rapidly varied flows, the friction can be neglected compared with pressure difference. Therefore, the present experimental setup, in terms of friction, does not limit one to apply the results to prototype flows. Nevertheless, in terms of flowrate through a bridge, one must treat the present experiments and prototype flows differently. For the present experimental setup, since the undeveloped boundary layers were very thin compared with the flow depth and channel width, one can approximate the velocity distribution of approach flows to be uniform.

4.3 3-Dimensional Scour Morphology and Width-averaged 2-Dimensional Longitudinal Scour Profiles

The major result of this study is the time-dependent variations of 3-dimentional scour morphology. Figure 4.3 and Figure 4.4 show the representations of the 3-dimensional scour processes at different times, the experimental conditions are h_b=13 cm, d_{50} =2 mm and h_b = 13 cm, d_{50} = 1 mm respectively. Corresponding width –averaged longitudinal scour profiles are shown in Figure 4.5 and Figure 4.6.

As was expected, since the larger grain is harder to move, the average maximum scour depths of the d_{50} =2 mm are less than that of the d_{50} =1 mm under all the conditions,

that means the scour decreases with increasing sediment size. All the four figures show that: (1) The shape of the scour holes remains almost unchanged as time elapses. The longitudinal scour profiles are bell-shaped curves, but not symmetrical because the eroded materials deposit approximately two to three times the deck width downstream of the bridge. (2) The scour hole develops rapidly from $t = 0$ to 0.5 hrs, which means the rate of change of scour depth is very large at the beginning of scour. (3) The scour depth increases as time elapses, but at $t = 30 \sim 42$ hrs, the change of scour depth is negligible, and the rate of change tends to zero, which implies that an equilibrium scour hole was attained approximately at $t = 30 - 42$ hrs. (4) The position of the maximum scour depth is close to the outlet of the bridge, at $x = -0.5$ to 0 cm, where $x = 0$ is 4 cm from the downstream face of the bridge. (5) In general, the scour morphology is approximately 2-dimensional before the maximum scour depth (because of pressurized flow) but 3-dimensional after the maximum scour depth (because of the effect of free-surface).

The figure 4.7 illustrates the representations of the 3-dimensional scour processes at different times, the experimental conditions are h_b =19 cm, d_{50} =1 mm. Corresponding width–averaged longitudinal scour profiles are shown in Figure 4.8. The scour increases as the bridge opening height, h_b, decreases, which means the scour increases with the deck inundation level, h_u - h_b.

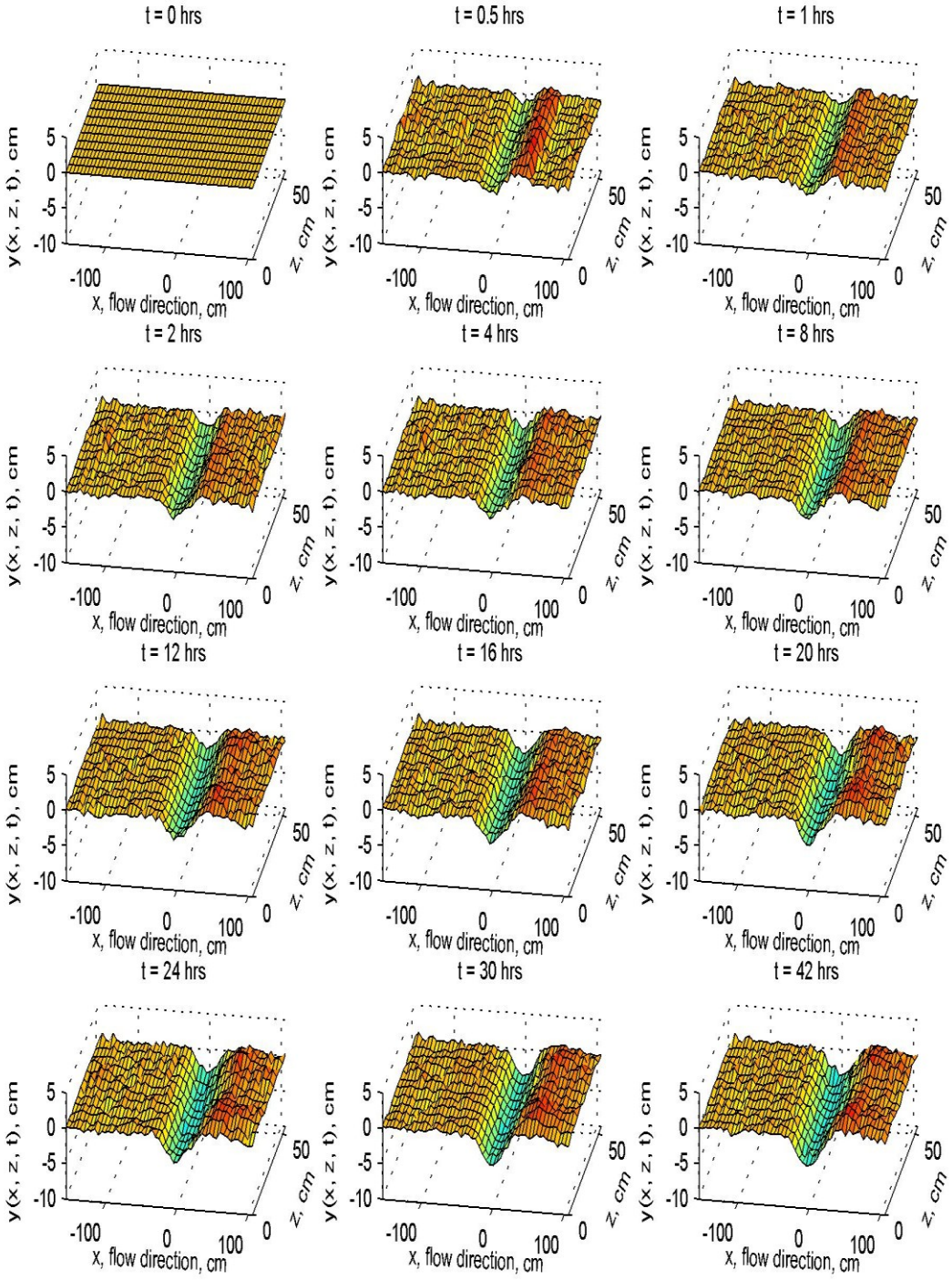

Figure 4.3 Representation of scour evolution at different times for h_b = 13 cm and d_{50} = 2 mm

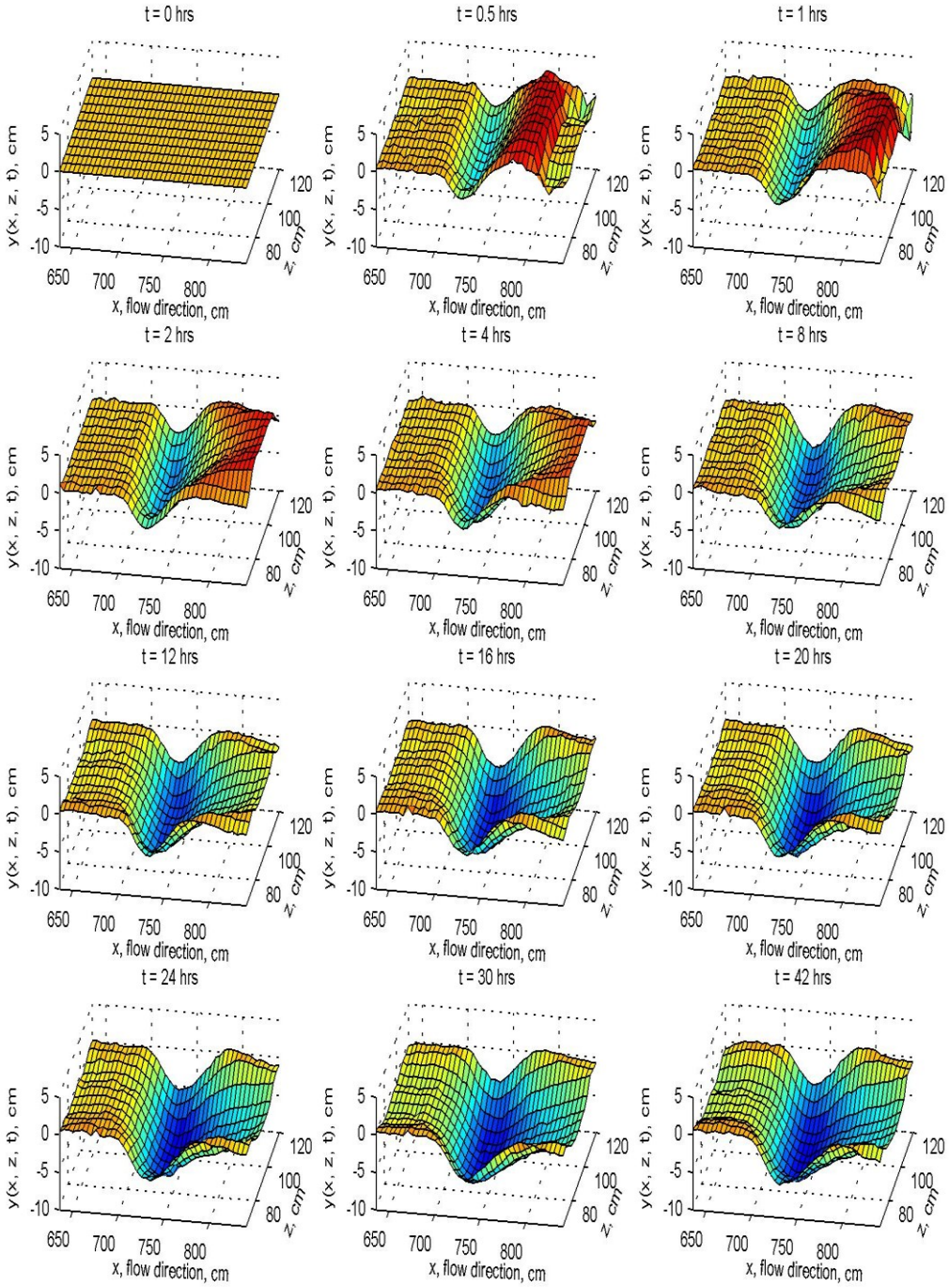

Figure 4.4 Representation of scour evolution at different times for h_b = 13 cm and d_{50} = 1 mm

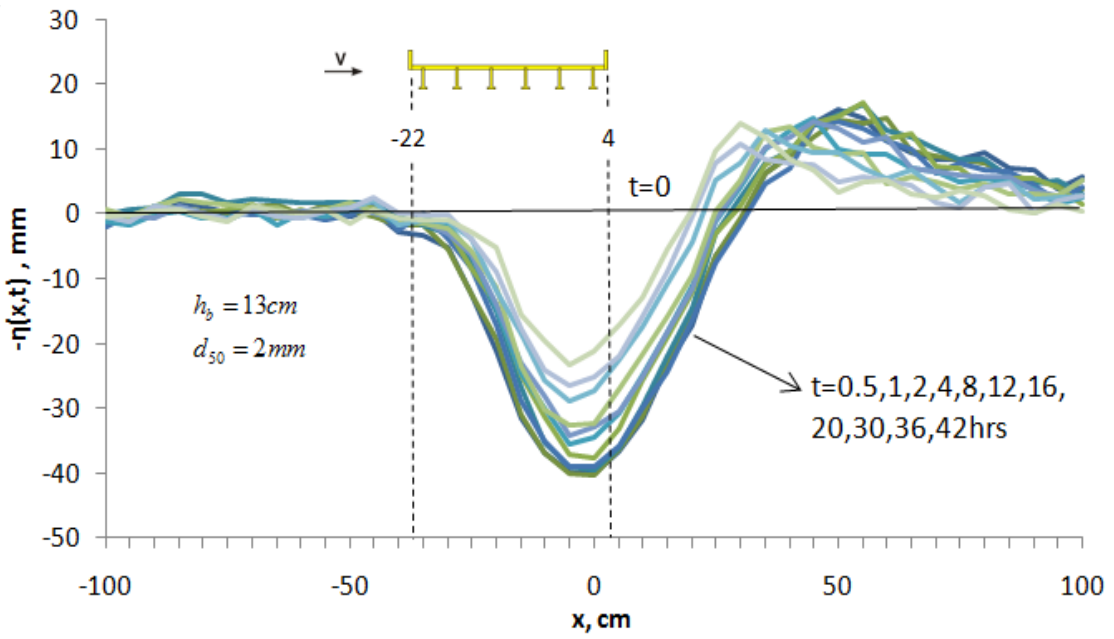

Figure 4.5 Evolution of width-averaged longitudinal scour profiles for h_b = 13 cm and d_{50} = 2 mm

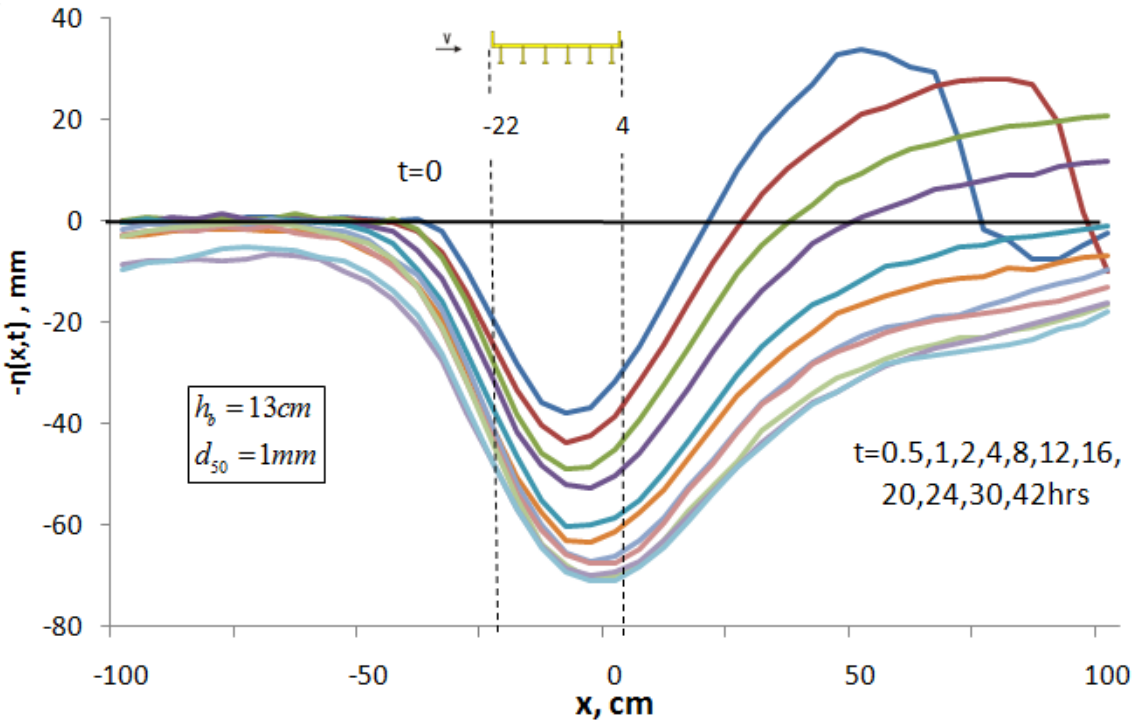

Figure 4.6 Evolution of width-averaged longitudinal scour profiles for h_b = 13 cm and d_{50} = 1 mm

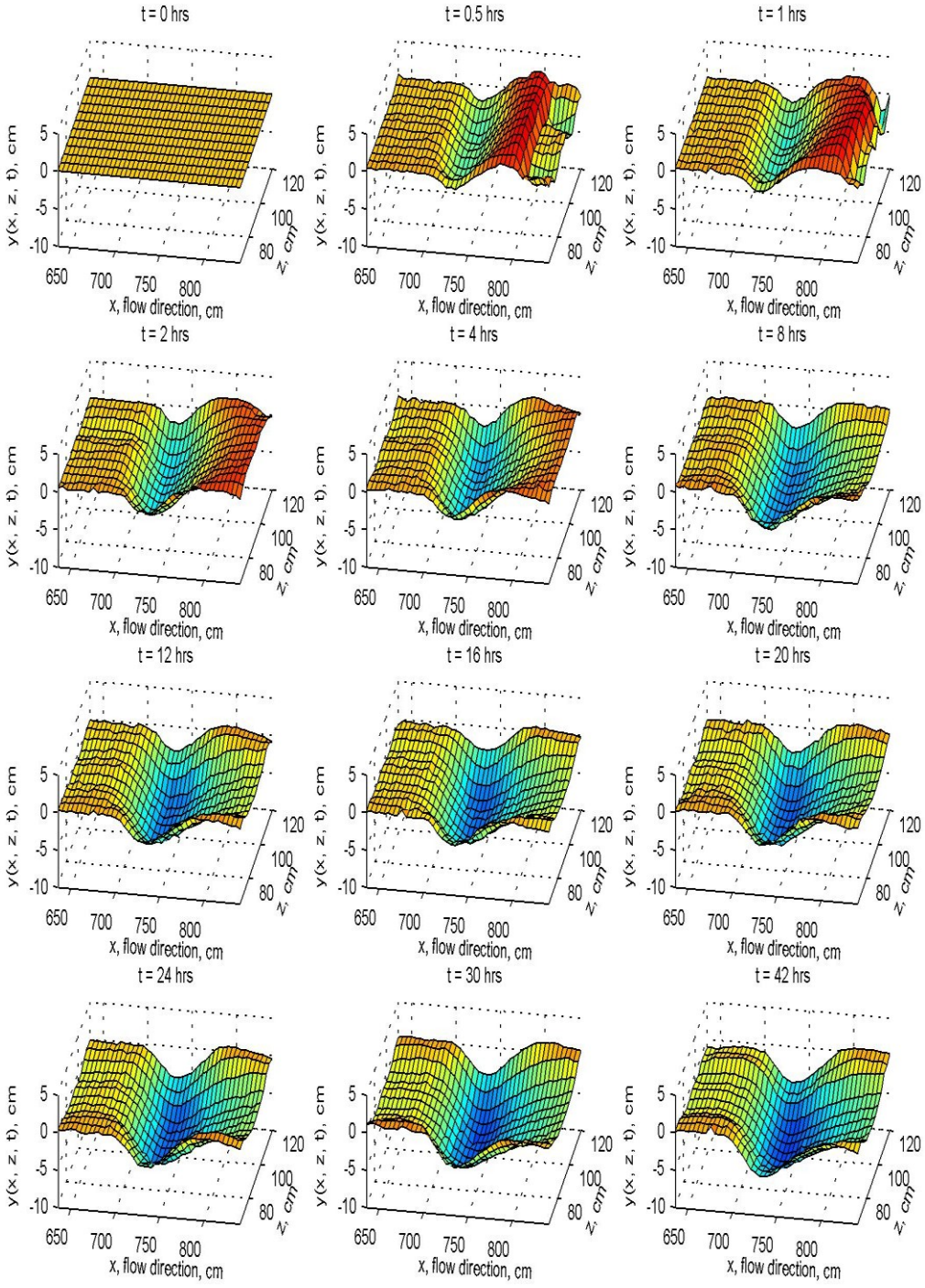

Figure 4.7 Representation of scour evolution at different times for h_b = 19 cm and d_{50} = 1 mm

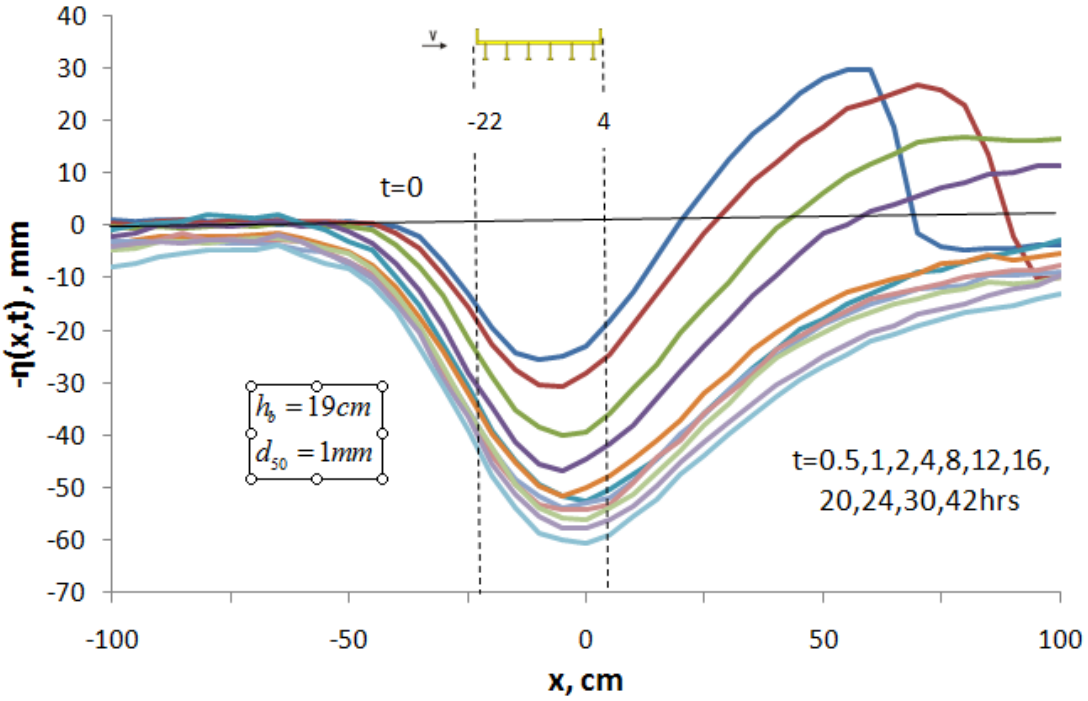

Figure 4.8 Evolution of width-averaged longitudinal scour profiles for h_b = 19 cm and d_{50} = 1 mm

4.4 Width-averaged Maximum Scour Depths

In terms of engineering concerns, the most important is the time-dependent variation of the maximum scour depths, which are summarized in Tables 4.1 and 4.2. Columns 1 and 2 in both tables were plotted in Fig.4.9 that again shows as time elapses, the maximum scour depth, $\eta(t)$, increases but the rate of change (slope) decreases and tends to zero as an equilibrium scour approaches. Further discussion of the maximum scour depths is addressed in the next chapter.

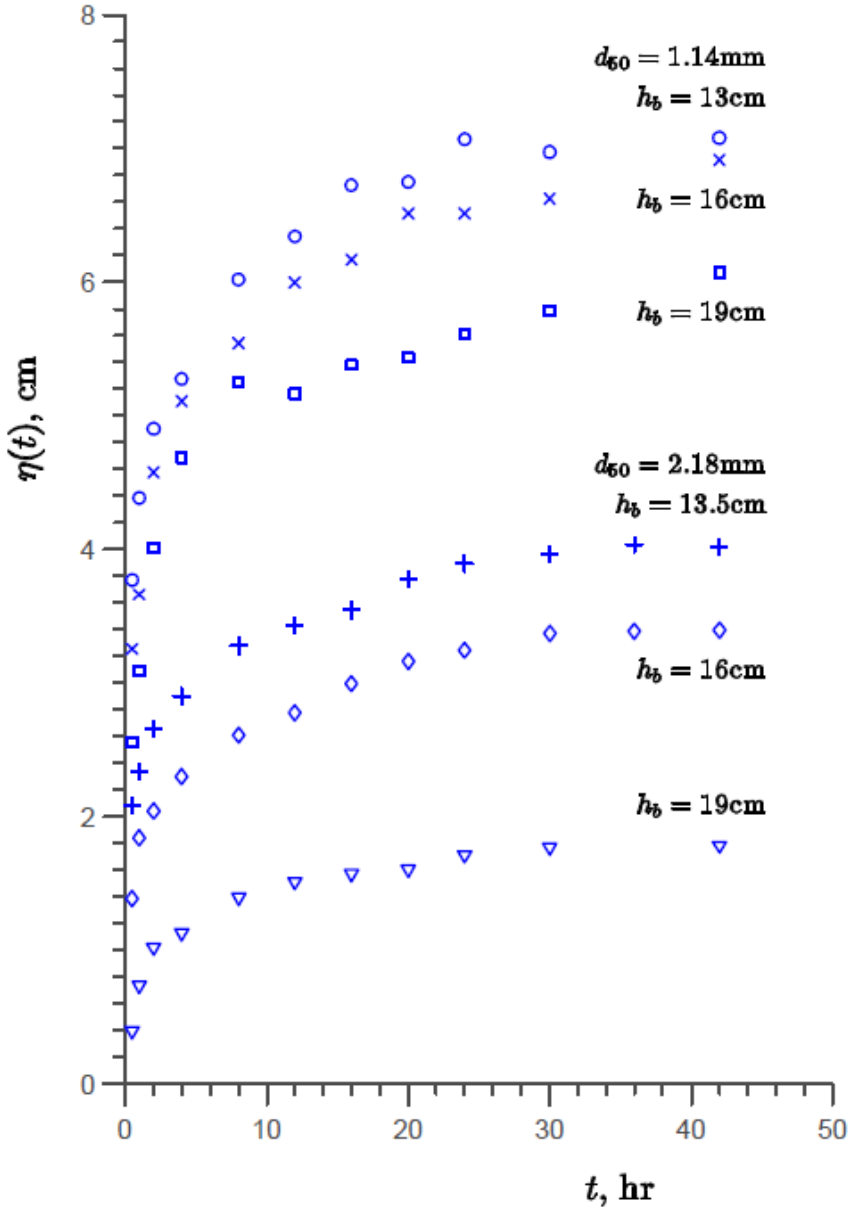

Figure 4.9 Variation of maximum scour depth $\eta(t)$ against time t

Table 4.1 Data of maximum scour depth against time for sediment d_{50} = 1.14mm

Time t (hr) (1)	Measured Scour Depth $\eta(t)$ (cm) (2)	(1) $\frac{tV_u}{h_b}$ $(\times 10^5)$ (3)	(2) $\frac{\eta(t)}{y_s}$ (4)	Calculated Scour Depth $\eta(t)$ (cm) (5)	Error (5)-(2) (cm) (6)
		$h_b = 13\,\text{cm}$			
0.5	3.77	0.06	0.532	3.28	-0.49
1	4.38	0.12	0.619	3.89	-0.49
2	4.90	0.24	0.692	4.51	-0.40
4	5.28	0.47	0.745	5.12	-0.16
8	6.02	0.94	0.850	5.73	-0.29
12	6.34	1.41	0.896	6.08	-0.26
16	6.73	1.88	0.950	6.32	-0.40
20	6.75	2.36	0.953	6.50	-0.26
24	7.07	2.83	0.998	6.62	-0.45
30	6.97	3.53	0.985	6.74	-0.23
42	7.08	4.95	1.000	6.76	-0.32
		$h_b = 16\,\text{cm}$			
0.5	3.25	0.05	0.470	3.02	-0.23
1	3.66	0.10	0.529	3.62	-0.04
2	4.58	0.19	0.662	4.22	-0.35
4	5.11	0.38	0.738	4.82	-0.29
8	5.54	0.77	0.802	5.42	-0.13
12	6.00	1.15	0.867	5.76	-0.23
16	6.17	1.53	0.892	6.01	-0.16
20	6.51	1.91	0.942	6.19	-0.33
24	6.51	2.30	0.942	6.33	-0.19
30	6.62	2.87	0.958	6.48	-0.15
42	6.92	4.02	1.000	6.62	-0.29
		$h_b = 19\,\text{cm}$			
0.5	2.55	0.04	0.420	2.52	-0.03
1	3.09	0.08	0.508	3.05	-0.04
2	4.01	0.16	0.661	3.58	-0.43
4	4.69	0.32	0.772	4.10	-0.58
8	5.25	0.64	0.865	4.63	-0.63
12	5.16	0.97	0.850	4.93	-0.23
16	5.38	1.29	0.886	5.15	-0.23
20	5.43	1.61	0.895	5.31	-0.12
24	5.61	1.93	0.924	5.44	-0.17
30	5.79	2.42	0.953	5.59	-0.20
42	6.07	3.38	1.000	5.76	-0.31

(1) V_u is the upstream velocity. h_b is the bridge opening height.
(2) The ratio of the scour depth with the maximum scour depth.

Table 4.2 Data of maximum scour depth against time for sediment d_{50} = 2.18mm

Time t (hr) (1)	Measured Scour Depth $\eta(t)$ (cm) (2)	(1) $\frac{tV_u}{h_b}$ $(\times 10^5)$ (3)	(2) $\frac{\eta(t)}{y_s}$ (4)	Calculated Scour Depth $\eta(t)$ (cm) (5)	Error (5)-(2) (cm) (6)
		$h_b = 13.5\,\text{cm}$			
0.5	2.08	0.07	0.516	1.44	-0.64
1	2.33	0.13	0.578	1.87	-0.46
2	2.66	0.27	0.659	2.30	-0.35
4	2.90	0.53	0.719	2.73	-0.17
8	3.28	1.07	0.812	3.16	-0.11
12	3.43	1.60	0.849	3.41	-0.02
16	3.54	2.14	0.878	3.57	0.03
20	3.78	2.67	0.936	3.69	-0.09
24	3.89	3.20	0.965	3.76	-0.13
30	3.97	4.00	0.984	3.82	-0.15
36	4.03	4.80	1.000	4.03	0
42	4.02	5.61	1.000	4.03	0.01
		$h_b = 16\,\text{cm}$			
0.5	1.38	0.05	0.408	1.11	-0.28
1	1.84	0.11	0.543	1.47	-0.37
2	2.04	0.22	0.602	1.83	-0.21
4	2.30	0.43	0.678	2.19	-0.11
8	2.61	0.87	0.769	2.55	-0.06
12	2.78	1.30	0.818	2.76	-0.01
16	2.99	1.74	0.882	2.90	-0.09
20	3.16	2.17	0.931	3.01	-0.15
24	3.24	2.60	0.956	3.09	-0.15
30	3.37	3.25	0.993	3.17	-0.20
36	3.38	3.90	0.998	3.21	-0.17
42	3.39	4.55	1.000	3.22	-0.18
		$h_b = 19\,\text{cm}$			
0.5	0.39	0.05	0.220	0.53	0.14
1	0.73	0.09	0.411	0.72	-0.01
2	1.02	0.18	0.570	0.91	-0.10
4	1.13	0.37	0.631	1.10	-0.02
8	1.39	0.73	0.781	1.29	-0.10
12	1.51	1.10	0.846	1.40	-0.10
16	1.57	1.46	0.879	1.48	-0.09
20	1.60	1.83	0.897	1.54	-0.06
24	1.71	2.19	0.958	1.58	-0.12
30	1.77	2.74	0.991	1.63	-0.13
42	1.78	3.84	1.000	1.69	-0.10

(1) V_u is the upstream velocity. h_b is the bridge opening height.
(2) The ratio of the scour depth with the maximum scour depth.

4.5 Summary

The change with time in maximum local scour depth from plane-bed to equilibrium conditions was recorded and analyzed. The experimental results include the velocity distributions of the approach flow, the records of 3-dimensional scour morphology, the width-averaged 2-dimensional longitudinal scour profiles, and the width-averaged maximum scour depths. Furthermore, in this study, the temporal development of scour on the pressurized flow river bed was experimentally studied using a physical hydraulic model. The study was performed under clear-water conditions using the uniform bed material and a 6 – gird deck. The principal objective of this research was to calculate the time development of the scour at the river bed until it reached the condition of equilibrium scour. Furthermore, in order to enlighten the underlying mechanisms responsible for the scour, the analysis of the effect of the sediment size, the open height of the bridge and the flow velocity was studied.

Chapter 5 Semi-empirical Model

5.1 Introduction

Prediction of local scour that develops downstream of hydraulic structures plays an important role in hydraulic design procedures. For any engineering work, designers should concern both safety and economy. While underestimation of the scour depth leads to the design of too shallow a bridge foundation, on the one hand, overestimation leads to uneconomical design on the other. Therefore, knowledge of the anticipated maximum depth of scour for a given discharge is a significant criterion for the proper design of a bridge pier foundation.

Scour depth can be determined by various methods, i.e. by use of empirical formulae, physical models and theoretical approaches. Traditionally, scour formation is estimated with the complete empirical formulae, mostly developed from experimental data. This approach is often unreliable and not representative because of neglecting some of the basic physics involved. Most of the empirical equations are based on the data of the laboratory models, or derived from the field data of certain rivers. Although the construction of these equations is simple and straightforward, much underlying hypothesis makes the equations are too subjective, and the full understanding of the scour process and the interaction of the various parameters are still incomplete. As a result, most of the empirical equations are only applicable for a limited range of hydraulic and geometric conditions.

In order to overcome the limitations of empirical models, it's natural to investigate the underlying mechanisms of the physical process and develop a general theoretical model incorporating all important factors. Such a model reflects the intrinsic characteristics of the system and describes the evolution of the dynamics. However, there are some inevitable difficulties with those theoretical models. First of all, the basic assumptions of the physical systems, which are the foundation of the theoretical models, might make the models inapplicable or inappropriate in reality. Hence, sometimes generalization or modification is necessary from a practical point of view. Second, it's always too soon to claim we have unveiled the full mechanism of the physical systems. A lot of work is still needed before we can fully understand the problems at hand.

This study presents a design method for time-dependent scour depth under bridge-submerged flow. After laboratory experiments were conducted to measure bridge-submerged local scour in different arrangements, experimental data were compiled for each arrangement to develop new semi-empirical equations based on the mass conservation of sediment. The proposed method can appropriately reduce the design depth of bridge scour according to design flow and a peak flow period, which can translate into significant savings in the construction of bridge foundations.

5.2 Semi-empirical Model for Maximum Scour Depth

Scour processes are described by the conservation of mass of sediment, which is often called the Exner equation (Paola and Voller 2005):

$$-c_b \frac{\partial \eta}{\partial t} + \nabla \cdot \mathbf{q}_s = 0 \tag{5.1}$$

where c_b = bed materials concentration or sediment packing density that can also be expressed as $(1-\lambda_p)$ in which λ_p is the bed porosity, η = scour depth at time t, the negative sign(-)is used since the positive direction of scour depth, η, is defined downward (Fig.5.1), and $\mathbf{q}_s$ = sediment flux (sediment discharge per unit area). The Exner equation states that scour depth, η, increases proportionally to the amount of sediment that is moved by the flow. For one-dimensional flow, after integrating over a flow cross-section, Eq. (5.1) reduces to:

$$-c_b \frac{\partial \eta}{\partial t} + \frac{\partial q_s}{\partial x} = 0 \tag{5.2}$$

where q_s = volumetric sediment transport rate per unit width, and x = coordinate in the flow direction. Assume that scour processes in clear water are mainly due to bedload transport, the sediment transport rate, q_s, in Eq. (5.2) can then be approximated by the Meyer-Peter equation (Chien and Wan, 1999)

$$\frac{q_s}{\sqrt{(s-1)gd_{50}^3}} = 8\left(\frac{\tau_0 - \tau_c}{(s-1)\rho g d_{50}}\right)^{3/2} \tag{5.3}$$

where s = specific gravity of sediment, g = gravitational acceleration, d_{50} = diameter of sediment, $\tau_0 = \tau_0(x,t)$ = bed shear stress varying with location x and time t, τ_c = critical shear stress for bedload motion, and ρ = density of water.

Substituting Eq. (5.3) into Eq. (5.2) and rearranging gives:

$$\frac{\partial \eta}{\partial t} = \frac{12}{(s-1)c_b}\sqrt{\frac{\tau_0 - \tau_c}{\rho}}\left(\frac{1}{\rho g}\frac{\partial \tau_0}{\partial x}\right) \tag{5.4}$$

where:

$$\tau_0 = \frac{f}{8}\rho V_b^2 \tag{5.5}$$

in which f = friction factor that varies with a Reynolds number and relative roughness, and V_b = cross-sectional average velocity under a bridge, which varies spatially and temporally. Eqs. (5.4) and (5.5) show that the rate of change of scour depth depends on the flow condition, $V_b(x,t)$, and sediment (packing density c_b, critical shear stress τ_c, and friction factor f). At the beginning of a scour process, $t=0$, the value of $\partial\eta/\partial t$ is large and positive since $\tau_0 > \tau_c$ and $\partial\tau_0/\partial x > 0$ (because downstream transport rate is always larger during a scour phase); after that, the value of $\partial\eta/\partial t$ decreases with time since both $\tau_0 - \tau_c$ and $\partial\tau_0/\partial x$ decrease with time; finally, the value of $\partial\eta/\partial t$ becomes zero when an equilibrium scour depth is attained. Accordingly, the temporal variation of the rate of change of scour depth, $\partial\eta/\partial t$, can be represented by the solid line in Fig. 5.2 where t_e = equilibrium time.

Theoretically, the solution of Eq. (5.4) must be coupled with a flow equation that describes the spatial and temporal variation of velocity $V_b(x,t)$ under a bridge. Nevertheless, the nonlinear interaction between scour depth and velocity under a bridge makes an exact solution for η impossible. For engineering concern, this analysis focuses on the temporal variation at the maximum scour depth where $x=0$, i.e. $\eta=\eta(0,t)$. According to Fig.5.2, as a first approximation in the middle of a scour phase, one can hypothesize that:

$$\frac{\partial\eta}{\partial t} \propto \frac{y_s}{t} \tag{5.6}$$

where the equilibrium scour depth y_s, which is related to flow conditions and has been discussed in Guo et al. (2009), is introduced since it is an appropriate scaling length of

scour depth η. Eq. (5.6) is represented by the dashed line in Fig.5.2 but it is not valid at $t = 0$ and $t = t_e$. Eq. (5.6) may be rewritten as

$$\frac{\partial \eta}{\partial t} = \frac{k y_s}{t} \tag{5.7}$$

where the constant k reflects the effect of sediment, as suggested by c_b, τ_c and f in Eqs. (5.4) and (5.5).

As for the packing density c_b, according to Chien and Wan (1999, p39), the porosity λ_p of sediment decreases with increasing sediment size d_{50}. In other words, the packing density c_b increases with increasing sediment size d_{50}. One then has the following reasoning:

$$d_{50}(\uparrow),\ c_b(\uparrow) \overset{\text{Eq.(5.4)}}{\Rightarrow} \frac{\partial \eta}{\partial t}(\downarrow) \overset{\text{Eq.(5.7)}}{\Rightarrow} k(\downarrow) \tag{5.8}$$

Similarly, for cohesionless sediment, the effect of critical shear stress τ_c can be reasoned as follows:

$$d_{50}(\uparrow),\ c_b(\uparrow) \overset{\text{Eq.(5.4)}}{\Rightarrow} \frac{\partial \eta}{\partial t}(\downarrow) \overset{\text{Eq.(5.7)}}{\Rightarrow} k(\downarrow) \tag{5.9}$$

Nevertheless, for the friction factor f, one has

$$d_{50}(\uparrow),\ f(\uparrow) \overset{\text{Eq.(5.5)}}{\Rightarrow} \tau_0(\uparrow) \overset{\text{Eq.(5.4)}}{\Rightarrow} \frac{\partial \eta}{\partial t}(\uparrow) \overset{\text{Eq.(5.7)}}{\Rightarrow} k(\uparrow) \tag{5.10}$$

Eqs. (5.8) and (5.9) show that the value of k decreases with increasing sediment size, but Eq. (5.10) states that the value of k increases with increasing sediment size. For natural sediments, the packing density varies between 50% and 75% (Chien and Wan 1999). In the early phase of a scour process, the shear stress τ_0 is much larger than that of

critical value τ_c. Therefore, the effects in Eqs.(5.8) and (5.9) may not be significant in an early phase of a scour process. As a result, the value of k may increase with increasing sediment size d_{50}. This hypothesis will be tested in the next section.

Integrating Eq. (5.7) and rearranging it gives:

$$\frac{\eta}{y_s} = k \ln t + B \tag{5.11}$$

where the integration constant B is approximately determined by the equilibrium condition, $\eta = y_s$ at $t = t_e$. Substituting this condition into Eq. (5.11) results in:

$$B = 1 - k \ln t_e \tag{5.12}$$

Eq. (5.11) then becomes:

$$\frac{\eta}{y_s} = k \ln \frac{t}{t_e} + 1 \tag{5.13}$$

which means in the middle of a scour process, the evolution of scour depth approximately follows a log law, like the law of wall in turbulent boundary layers.

Note that although the constant B in Eq. (5.12) is determined at $t = t_e$, Eq. (5.13) should not be valid at $t = 0$ and $t = t_e$ since the hypothesis, Eq. (5.6), is not valid there, as shown in Fig. 5.2. Fortunately, the scour depth at $t = 0$ is insignificant in practice so that one can ignore this flaw, like the log law velocity profile at a rough wall. The second flaw at $t = t_e$ can be fixed by analogizing it to the modified log-wake law in turbulent boundary layers (Guo and Julien 2003, Guo et al. 2005), which means one can force the rate of change of scour depth to be zero at $t = t_e$ by adding a cubic function to Eq. (5.13), i.e.

$$\frac{\eta}{y_s} = k\left[\ln\frac{t}{t_e} - \frac{1}{3}\left(\frac{t}{t_e}\right)^3 + \frac{1}{3}\right] + 1 \tag{5.14}$$

where the equilibrium time t_e is characterized by the overall flow conditions and may be expressed by

$$t_e = C\frac{h_b}{V_u} \tag{5.15}$$

where C is an undetermined constant, h_b = bridge opening height before scour (Fig. 5.1), and V_u = approach velocity upstream of a bridge. Substituting Eq. (5.15) into Eq. (5.14) gives:

$$\frac{\eta}{y_s} = k\left[\ln\frac{tV_u}{Ch_b} - \frac{1}{3}\left(\frac{tV_u}{Ch_b}\right)^3 + \frac{1}{3}\right] + 1 \tag{5.16}$$

which is called the log-cubic law for temporal variation of submerged-flow bridge scour.

Finally, one can summarize the above with the following hypothesis: Time-dependent scour depth may be described by a log-cubic law, Eq. (5.16), where the scour depth η is scaled by its equilibrium depth y_s, the time t is scaled by the approach velocity V_u and bridge opening height h_b, and the parameter k may increase with increasing sediment size while the parameter C may be a universal constant.

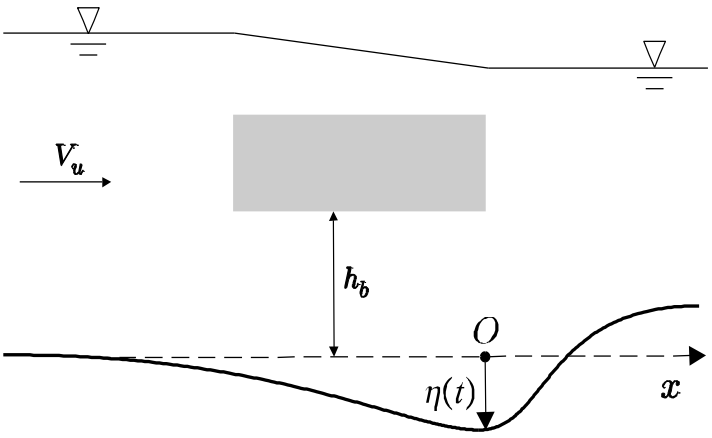

Figure 5.1 Coordinate system for sediment continuity equation

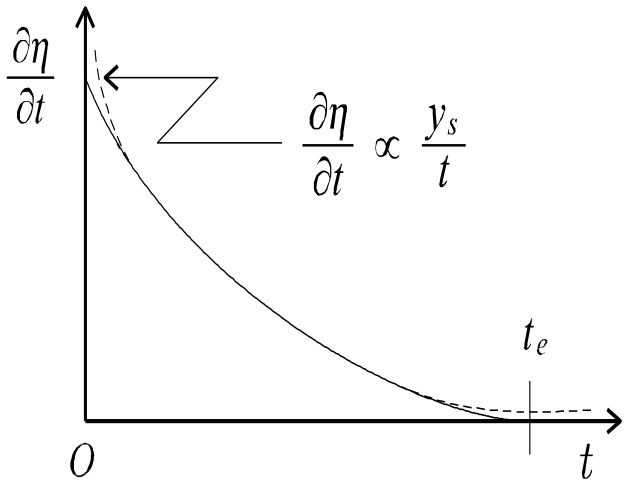

Figure 5.2 Characteristics of rate of change of scour depth

5.3 Test of Semi-empirical Model

To test the hypothesis, the present experimental data are, first, plotted according to η / y_s versus tV_u / h_b in Fig.5.3, which demonstrates that the scour depth η and time t are indeed appropriately scaled by y_s and h_b / V_u, respectively.

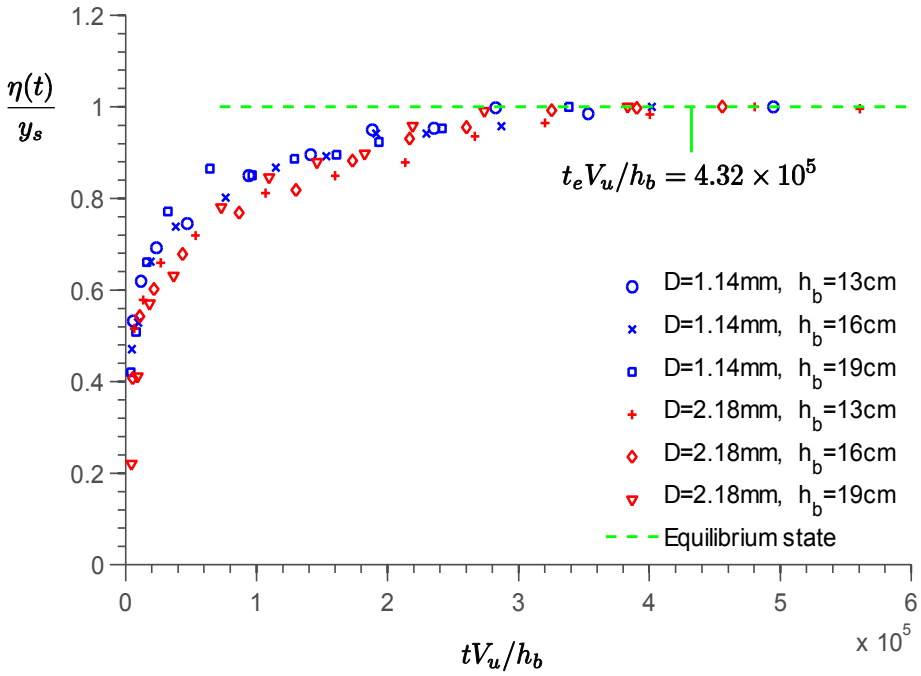

Figure 5.3 Test of similarity hypothesis and determination of universal constant C

The equilibrium state is, next, read from Fig.5.3 where

$$\frac{t_e V_u}{h_b} \approx 4.32 \times 10^5 \tag{5.17}$$

which gives the constant C in Eq. (5.15) as

$$C \approx 4.32 \times 10^5 \tag{5.18}$$

One can, then, clearly see from Fig.5.3 that most of the data points for $d_{50} = 1.14\,\text{mm}$ (blue) are above those for $d_{50} = 2.18\,\text{mm}$ (red), which just confirms the hypothesis that the value of k increases with increasing sediment size (since the value in the brackets of Eq. (5.16) is negative). Furthermore, using a nonlinear least-squares method in MatLab, fitting Eq. (5.16) to the present data gives:

$$\begin{aligned} k &= 0.125 \quad \text{for } d_{50} = 1.14\,\text{mm} \\ k &= 0.154 \quad \text{for } d_{50} = 2.18\,\text{mm} \end{aligned} \tag{5.19}$$

which are shown in Fig. 5.4 through the slopes. Finally, the model parameters in Eqs. (5.18) and (5.19) can well fit the log-cubic law, Eq. (5.16), to the data of the columns 3

and 4 in Tables 4.1 and Table 4.2 of chapter 4, shown in Fig.5.5 and Fig.5.6 for $d_{50} = 1.14\,\text{mm}$ and $d_{50} = 2.18\,\text{mm}$, respectively. The corresponding correlation coefficients, R^2, and standard deviations, σ, are as follows:

$$\begin{aligned} R^2 &= 0.982, \quad \sigma = 0.030, \quad \text{for } d_{50} = 1.14\,\text{mm} \\ R^2 &= 0.963, \quad \sigma = 0.036, \quad \text{for } d_{50} = 2.18\,\text{mm} \end{aligned} \tag{5.20}$$

Assume a Gaussian distribution for the regression errors. This results implies that for $d_{50} = 1.14\,\text{mm}$, 68% of the regression errors fall into the interval $(0 \pm \sigma) = \pm 0.03$. In other words, with a 68% confidence interval, the estimated scour depth has an error of $\pm(3-4)\%$ of equilibrium scour depth y_s. Similarly, with a 95% confidence interval, the estimated scour depth has an error of $\pm(6-7)\%$ of equilibrium scour depth y_s. Besides, the absolute errors between the proposed model and the measured maximum scour depths are tabulated in the column 6 in Tables 2 and 3, where the maximum error is about $6\,\text{mm}$ (the first row of data in Table 4.2) that is within the usual uncertainties of bedform measurements in flume experiments.

One can conclude that the log-cubic law, Eq. (5.16), indeed describes the time-dependent scour depth under bridge-submerged flow where the parameter C is a universal constant, but the parameter k increases with increasing sediment size. Because of the limitation of sediment sizes in the present experiments, a general relationship between the parameter k and sediment size d_{50} cannot be generated in this study.

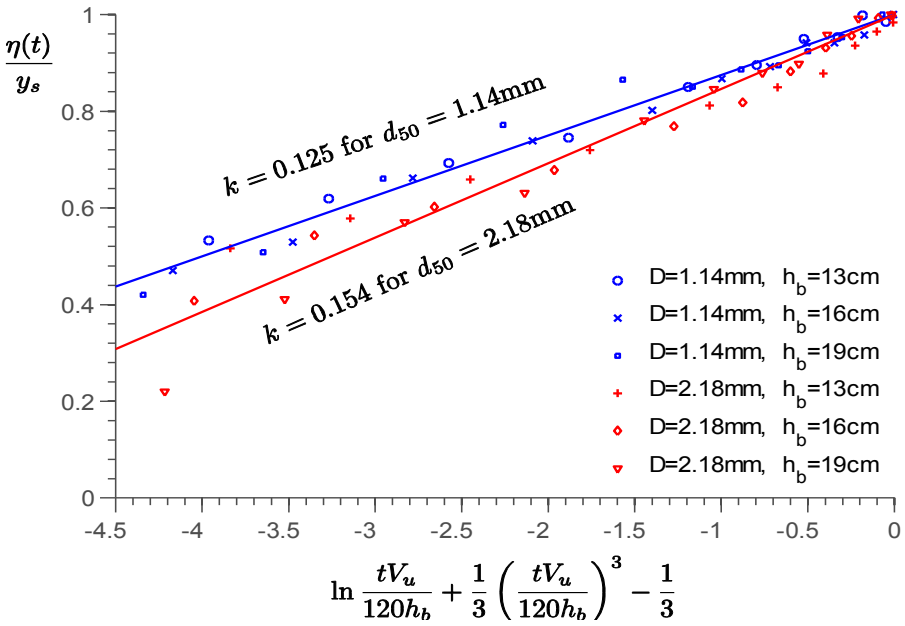

Figure 5.4 Variation of parameter k with sediment size d_{50}

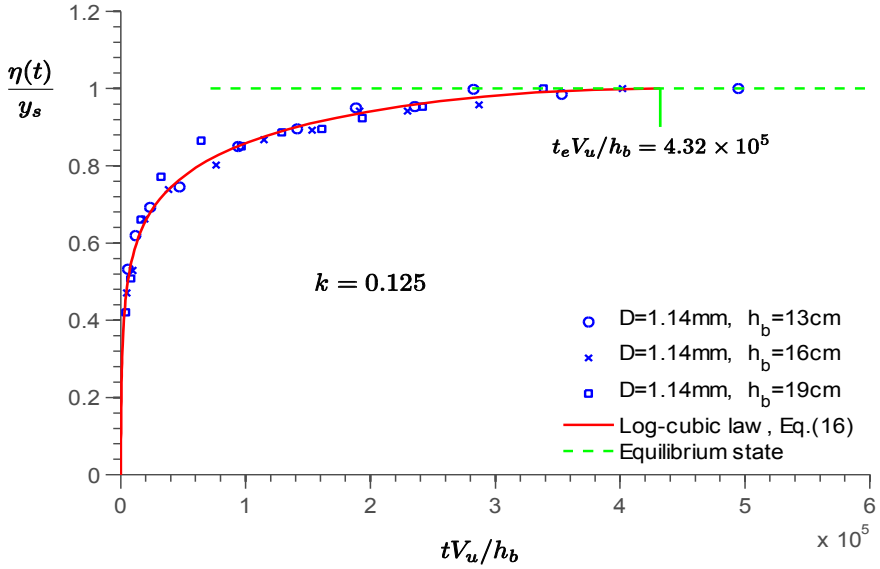

Figure 5.5 Test of log-cubic law with data of d_{50} = 1 mm

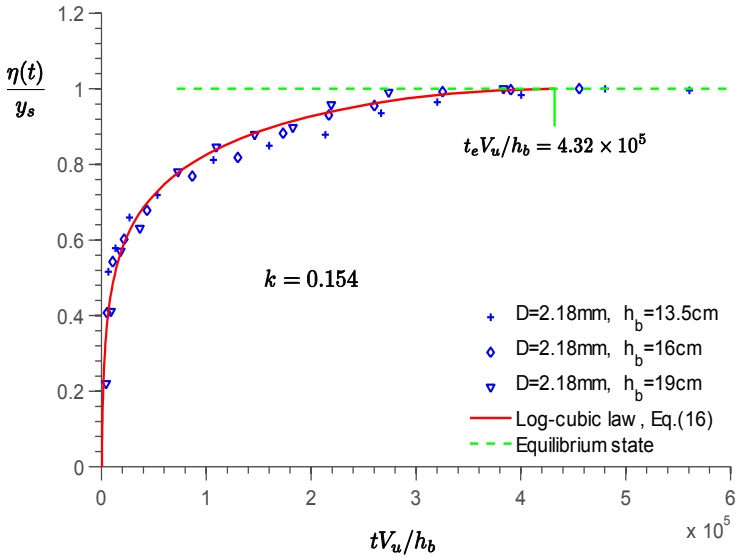

Figure 5.6 Test of log-cubic law with data of d_{50} = 2 mm

Chapter 6 Conclusion and Future Work

6.1 Conclusions

The results of the experimental study reveal the following:

- The depth of scour is highly dependent on time. The depth of scour hole increases as the time increases until equilibrium state.
- The shape of the longitudinal scour profiles remains almost unchanged with respected to time.
- The position of the maximum scour depth quickly moves to its equilibrium position that is close to the downstream edge of the bridge deck.
- The rate of change of scour depth decreases as time elapses and tends to be zero as the scour approaches its equilibrium state.
- The maximum scour depth can be described by two similarity numbers where the time-dependent scour depth is scaled by the corresponding equilibrium scour depth, and the time by the approach velocity and bridge opening height, as shown in Figure 5.3 of Chapter 5.
- The time-dependent scour depth can be estimated by the log-cubic law, Eq. (5.16)

$$\frac{\eta}{y_s} = k\left[\ln\frac{tV_u}{Ch_b} - \frac{1}{3}\left(\frac{tV_u}{Ch_b}\right)^3 + \frac{1}{3}\right] + 1$$

which agrees very well with the collected flume data (Figure 5.5 and Figure 5.6).

- The proposed method may be used to estimate the evolution of scour depth at a certain time, which can appropriately reduce the design depth and construction cost of a bridge foundation according to design flow and peak flow duration.

6.2 Implication and Limitation

Current practice for determining the scour depth at a bridge crossing is based on the equilibrium scour depth of a design flood (e.g., 50-year, 100-year, and 500-year flood events), which is unnecessarily larger than a real maximum scour depth during a bridge life span since the peak flow duration of a flood event is often much shorter than its equilibrium time. The proposed method can be used to estimate the evolution of scour depth at a certain time, which means it can appropriately reduce the design depth and construction cost of a bridge foundation according to design flow and a peak flow duration. Nevertheless, the proposed method is limited to steady flow with clear water conditions and uniform bed materials.

In addition, when applying Eq. (5.16) to practice, one has to note that: (1) the equilibrium scour depth y_s is estimated by Guo et al. (2009) although the measured values were used in the present study; and (2) the proposed method is only valid for

$$\frac{tV_u}{h_b} \le 4.32 \times 10^5$$

when $tV_u / h_b > 4.32 \times 10^5$, the equilibrium scour depth is used where $\eta = y_s$

6.3 Future Work

Recommendations regarding possible future work in relation to the current research project are as bellows:

- Most of the research on scour has been conducted under free-surface flow condition with the resultant scour prediction equations based on free-surface flows (Lagasse et al. 1991; Richardson et al. 1993). Few study focus on the aspect of general scour under bridge-submerged flow condition (or pressurized flow condition). However, the bridge-submerged floods occur commonly in many regions. Present study is to compute pressure-flow scour independently of local scour (removing the pier), future work could develop a comprehensive model that would incorporate both scour phenomena.
- In this study, all the experiments were run below the incipient motion velocity for each sediment size, which means clear-water condition. Using the sediment recirculation equipment, live-bed experiments will be conducted in the next step of the study.
- Two sets of uniform sediment were used in this study. However, this is ideal condition in the lab. The future work should be focused on the investigation of scour depth for the non-uniform sediment, which has more practical significance.
- The semi-empirical equation of the temporal variation of scour depth in this study, should to be applied for the unsteady flow in the next work. The flow conditions, such as the flow velocity, flow pressure, acceleration affect the scour depth significantly.

REFERENCES

Ahmad, M. (1953). "Experiments on design and behavior of spur-dikes." *Proc. Int. Hydraul.* Convention., 145-159.

Anderson, A. G. (1963). "Sediment transportation mechanics:erosion of sediment." *J. Hydraul. Div., Am. Soc. Civ. Eng.* 89, 237-248.

Arneson, L. A., and Abt, S. R. (1998). "Vertical contraction scour at bridges with water flowing under pressure conditions." *Transportation Research Record*. 1647, 10-17.

Bailey et al., (2002). "Niveau de securite requis pour l'evaluation des ponts-routes existants." *Report Nr. 566*, Zurich.

Ballio, F., and Orsi, E. (2000). "Time evolution of scour around bridge abutments." *Water Engineering Research*, 1-17.

Barbhuiya, A. K. and Dey, S., (2004). "Local scour at abutments: a review." *Flow Meas. Instrum.,* 29(5), 449-476.

Barkdoll, B. D., Ettema R., and Melville B. W. (2007). "Countermeasures to protect bridge abutments from scour." *NCHRP Report 587*. Transportation Research Board.

Bateni, S. M., Jeng, D. S., Melville, B. W. (2007). "Bayesian neural networks for prediction of equilibrium and time-dependent scour depth around bridge piers." *Advances in Engineering Software*, 38, 102–111.

Bormann, N. E. and Julien, P. Y. (1991). "Scour downstream of grade-control structures." *J. Hydraul. Engrg*., 117(5), 579-594.

Breusers, H. N. C. (1967). "Time scale of two-dimensional local scour." *Proc. 12th Cong. IAHR,* 3, 275-282.

Breusers, H. N. C., and Raudkivi, A. J. (1991). "Scouring – Hydraulic structures design manual."

Breusers, H. N. C., Nicollet, G. and Shen, H. W. (1997). "Local scour around cylindrical piers." *J. Hydraul. Res.,* 15(3), 211-252.

Cardoso, A. H., and Bettess, R. (1999). "Effects of time and channel geometry on scour at bridge abutments." *J. Hydraul. Eng., Am. Soc. Civ. Eng.*, 125, 388-399.

Carstens, M. R. (1966). "Similarity laws for localized scour." *J. Hydraul. Div., Am. Soc. Civ. Eng.*, 92, 13-36.

Chabert, J. and Engeldinger, P. (1956). "Etude des affouillements autor des piles de points (Study of scour at bridge piers)." Bureau central d'Etudes les Equipment d' Outre-Mer, Laboratory National d' Hydraulique, France.

Chang, W. Y., Lai, J. S., and Yen, C. L. (2004). "Evolution of scour depth at circular bridge piers." *J. Hydraul. Res.*, 130(9), 905-913.

Chien, N., and Wan, Z. (1999). "Mechanics of Sediment Transport." ASCE Press.

Chiew, Y. M. and Melville, B. M. (1987). "Local scour around bridge piers." *J. Hydraul. Res*., 25(1), 15-26.

Coleman, S. E., Lauchlan, C. S. and Melville B. W., (2003). "Clear-water scour development at bridge abutments." *J. Hydraul. Res*., 41(5), 521–531.

Cunha, L. V., (1975). "Time evolution of local scour." Proceedings, 16th IAHR Congress, Sao Paulo, Brazil, July 27-Agust 1, 285-299.

Dargahi, B. (1990). "Controlling mechanism of local scouring." *J. Hydraul. Engrg.*, 116(10), 1197-1214.

David, K. M. (2000). "National bridge scour program-measuring scour of the streambed at highway bridges." *U.S. Geological Survey*, Reston, Va.

Dey, S. (1999). "Time-variation of scour in the vicinity of circular piers." *J. Water and maritime Engrg.,* 136(2), 67-75.

Dey, S., and Barbhuiya, A. K. (2004). "Clear-water scour at abutments in thinly armoured beds." *J. Hydraul. Engrg.,* 130(7), 622-634.

Dey, S., and Barbhuiya, A. K. (2005). "Time variation of scour at abutments." *J. Hydraul. Engrg.*, 131(1), 11-23.

Dey, S. and Sarkar, A. (2006). "Scour downstream of an apron due to submerged horizontal jets." *J.* Hydraul*. Engrg*., 132(3), 246–257.

Ettema, R. (1980). "Scour at bridge piers." *Report No.216*, University of Auckland, New Zealand.

Franzetti, S., Larcan, E., and Mignosa, P. (1982). "Influence of the test duration on the evaluation of ultimate scour around circular piers." *Proc. Int. Conf. Hydraulics and Modeling of Civil Structures*, Coventry, England, 381-396.

Garde, R. J., and Kothyari, U. C. (1998). "Scour around bridge piers." *PINSA*, 4, 569-580.

Gill, M. A. (1972). "Erosion of sand beds around spur-dikes." *J. Hydraul. Div. Am. Soc. Civ. Eng.* 98, 1587-1602.

Giri, S. and Shimizu, Y. (2005). "A method for local scour prediction at river structures considering time factor." *Annual Journal of Hydraulic Engineering*, JSCE, 49, 781-786.

Guo, J., and Julien, P. Y. (2003). "Modified log-wake law for turbulent flow in smooth pipes." *J. Hydraul. Res.*, 41(5), 493-501.

Guo, J., Julien, P. Y., and Meroney, R. N. (2005). "Modified log-wake law for zero-pressure-gradient turbulent boundary layer." *J. Hydraul. Res.*, 43(4), 421-430.

Guo, J., Kerenyi, K., Pagan-Ortiz, J., and Flora, K. (2009). "Submerged-flow bridge scour under maximum clear-water conditions." Submitted to *J. Hydraul. Engrg.*

Johnson, P. A., and McCuen, R. H., (1991). "A temporal spatial pier scour model." *Transportation Res. Record*, 1319, 143-149.

Kandasamy, J. K. (1989). "Abutment scour." *Rep. No.458, School of Engineering*, University of Auckland, Auckland, New Zealand.

Karim, O. A. and Ali, K. H. M. (2001). "Prediction of flow patterns in local scour caused by turbulent water jets." *J. Hydraul. Res.*, 38(4), 279-287.

Kattell, J., and Eriksson, M. (1998). "Bridge scour evaluation: screening, analysis, & countermeasures" *US Forest Service.*

Khwairakpam, P., and Mazumdar, A. (2009). "Local scour around hydraulic structures." *International Journal of Recent Trends in Engineering*, 1(6), 59-61.

Kohli, A., Hager, W. H., (2001). "Building scour in floodplains." *Water Maritime Eng., Inst. Civ. Eng.*, (London). 148, 61-80.

Kothyari, U. C., Garde, R. C., and Raju, K. G. R. (1992). "Temporal variation of scour around circular bridge piers." *J. Hydraul. Engrg.*, 118(8), 1091-1106.

Kraus, N., Lohrman, A., and Cabrera, R. (1994). "New acoustic meter for measuring 3D laboratory flows." *J. Hydraul. Engrg.*, 20(3), 406-412.

Lagasse, P. F., Richardson, E. V., Schall, J. D., Price, G. R. (1997). "Instrumentation for measuring scour at bridge piers and abutments." *NCHRP Report* 396*,* Transportation Research Board.

Lagasse, P. F., Clopper P. E., Zevenbergen L. W. and Girard, L. G., (2007). "Countermeasures to protect bridge piers from scour." *NCHPR Report 593,* Transportation Research Board.

Lai, J. S., Chang, W. Y., and Yen, Y. L. (2009). "Maximum local scour depth at bridge piers under unsteady flow." *J. Hydraul. Engrg.*, 135(7), 609-614.

Lauchlan, C. S. and Melville, B. W. (2001). "Riprap protection at bridge piers." *J. Hydraul. Engrg.*, 121(9), 635-643.

Laursen, E. M. (1952). "Observation on the nature of scour." *Proc. 5th Hydraul. Conf.*, 179-197.

Laursen, E. M. (1958). "Scour at bridge crossings." Bull. No. 8, Iowa Highways Research Board, Ames, Iowa.

LeBeau, K. H., Wadia-Fascetti, S. J. (2007). "Fault tree analysis of Schoharie creek bridge collapse." *J. Performance of Constructed Facilities*, 21(4), 320-326.

Lee, Y., Lee, J. S. (1998) "Estimation of scour depth at bridges and comparative analysis between estimated and measured scour depths." *Proc. 3rd Int. Conf. on Hydro-Science and Engineering.*

Lim, S. Y., (1997). "Equilibrium clear scour around an abutment." *J. Hydraul. Engrg.*,237-243.

Lohrman, A., Cabrera, R., and Kraus, N. (1994). "Acoustic Doppler velocimeter (ADV) for laboratory use." Proc. from symposium on fundamental and adv. in hydraulic measurement and experimentation, ASCE, 351-365.

Lopez, G., Teixeira, L., Ortega-Sanchez, M., and Simarro, G. (2006). "Discussion: Further results to time-*dependent* local scour at bridge elements." *J. Hydraul. Engrg.*, 132(9), 995-996.

Lu, J. Y., Hong, J. H., Su, C. C., Wang, C.Y. and Lai, J. S. (2008). "Field measurements and simulation of bridge scour depth variations during floods." *J. Hydraul. Engrg.*, 134(6), 810-821.

Lyn, D. A. (2008). "Pressure-flow scour: a re-examination of the HEC-18 equation." *J. Hydraul. Engrg.,* 134(7), 1015-1020.

Melville, B. W. and Raudkivi, A. J. (1977). "Flow characteristics in local scour at bridge piers." *J. Hydraul. Res*., 15(1), 373-380.

Melville, B. W. (1984). "Live bed scour at bridge piers." *J. Hydraul. Engrg*., 110(9), 1234-1247.

Melville, B. W. (1992). "Discussion: Study of time-dependent local scour around bridge piers." *J. Hydraul. Engrg.*, 118(11), 1593-1595.

Melville, B. W., and Chiew, Y. M. (1999). "Time scale for local scour at bridge piers." *J. Hydraul. Engrg.*, 125(1), 59-65.

Melville, B. W., and Coleman, S. E. (2000). "Bridge scour." *Water Res.,* LLC, Colorado, U.S.A., 550.

Mia, M. F. and Nago, H. (2003) "Design method of time-dependent local scour at circular bridge pier." *J. Hydraul. Engrg*., 129(6), 420-427.

Murillo, J. A. (1987). "The scourge of scour." *Civil Engineering*, 57(7), 66-69.

Neill, C. R. (1973). *Guide to bridge hydraulics*. University of Toronto Press.

Oliveto, G., and Hager, W. H. (2002). "Temporal evolution of clear water pier and abutment scour." *J. Hydraul. Engrg.*, 128(9), 811-820.

Oliveto, G., and Hager, W. H. (2005). "Further results to time-dependent local scour at bridge elements." *J. Hydraul. Engrg.*, 131(2), 97-105.

Pagliara, S., Hager, W. H., and Unger, J. (2008). "Temporal evolution of plunge pool scour." *J. Hydraul. Engrg*., 134(11), 1630–1638.

Paola, C., and Voller, V. R. (2005). "A generalized exner equation for sediment mass balance." *J. Geophys. Res.*, 110, 1-8.

Patrick, A. (2006). "Time development of local scour at a bridge pier fitted with a collar," MS thesis, Univ. of Saskatchewan, Canada.

Rajaratnam, N., Nwachukwu, B.A., (1983). "Flow near groin-like structures." *J. Hydraul. Engrg.,* 109, 463-480.

Raudkivi, A. J. and Ettema, R. (1983). "Clear-water scour at cylindrical piers." *J. Hydraul. Engrg*., 109(3), 339-350.

Rhodes, J., Trent, R. (1993). "Economics of floods, scour, and bridge failures." *J. Hydraul. Engrg.,* 93, 928-933.

Richardson, E. V. and Davies, S. R. (1995). "Evaluating scour at bridges." Rep. No.FHWA-IP-90-017 (HEC 18), Federal Administration, U.S. Department of Transportation, Washington, D.C..

Rouse, H. (1965). Engineering hydraulics: sediment transportation (New York: John Wiley and Sons).

Setia, B. (2008) "Equilibrium scour depth time." *Proc.3rd Iasme/Wseas Int. Conf. on Water Resources*, Hydraulics & Hydrology, 114-117.

Shen, H. W., Ogawa, Y. and Karaki, S. K. (1965), "Time variation of bed deformation near the bridge piers." *Proc. 11th Congress*, IAHR, 3-14.

Smith, D.W. (1976). "Bridge failures." *J. ICE Proceedings*. 60(3), 128.

SonTek. (1997). "Acoustic doppler velocimeter." *Technical documentation, version 4.0*.

Sumer, B. M., Fredsoe, J. and Christiansen, N. (1992). "Scour around vertical pile in waves." *J. Wtrwy., Port, Coast., and Oc. Engrg*., 118(1), 15-31.

Ting, F. C. K., Briaud, J. L., Chen, H. C., Gudavalli, R. and Perugu, S., (2001). "Flume tests for scour in clay at circular piers." *J. Hydraul. Engrg*., 127(11), 969-978.

Umberll, E. R., Young, G. K., Stein, S. M., and Jones, J. S. (1998) "Clear water contraction scour under bridge in pressure flow." *J. Hydraul. Engrg*.,124(2), 236-240.

Voulgaris, G., and Trowbridge, J. (1998). "Evaluation of the acoustic Doppler velocimeter for turbulence measurements." *J. Atmospheric and Oceanic Technology*. 15, 272-288.

Whitehouse, R. J. S. (1997). "Scour at marine structures." *Res. Rep. SR417*, HR Wallingford Limited, Wallingford, UK.

Yanmaz, A. M., and Altmbilek, H. D. (1991). "Study of time-dependent local scour around bridge piers." *J. Hydraul. Engrg.,* 117(10), 1247-1268.

Yanmaz, A. M. (2006). "Temporal variation of clear water scour at cylindrical bridge piers." *Can. J. Civ. Eng.*, 33, 1098-1102.

Yanmaz, A. M., and Kose, O. (2007). "Surface characteristics of scouring at bridge elements." *Tur.J. Eng. Env. Sci.,* 31, 127-134.

Yanmaz, A. M., and Kose, O. (2009). "A semi-empirical model for clear-water scour evolution at bridge abutments." *J. Hydraul. Res.*, 47(1), 110-118.

APPENDIX GLOSSARY

B = Integration constant;

C = Model constant for equilibrium time;

C_b = Bed materials concentration or sediment packing;

d_{50} = Median diameter of sediment;

Fr = Froude Number;

f = Friction factor;

g = The gravitational acceleration;

h_b = Bridge opening height before scour;

k = Model parameter reflecting effect of sediment size;

O = Origine of coordinate system;

q_s = Sediment flux;

q_s = Sediment transport rate per unit width;

R = Correlation coefficient;

R_e = Reynolds number based on hydraulic radius;

R_h = Hydraulic radius;

s = Specific gravity of sediment;

t = Time;

t_e = Equilibrium time;

V_b = Cross-sectional averaged velocity under a bridge;

V_u = Approach velocity in upstream of a bridge;

x = Coordinate in flow direction;

y = Coordinate in vertical direction;

y_s = Equilibrium scour depth;

z = Coordinate in lateral direction;

$\eta(x,t)$ = Scour profile at time;

$\eta(t)$ = Maximum scour depth at time;

λ_p = Bed porosity;

ρ = Density of water;

σ = Standard deviation;

τ_c = Critical shear stress for bedload motion;

τ_0 = Bed shear stress.